Downloaded from genome.cshlp.org on November 17, 2026 . Published by Cold Spring Harbor Laboratory Press



Liver X receptors participate in the fasting response by assisting CEBPB binding to enhancers and promoting the fasting transcriptional program

Tali Gorbonos, Maria C. Romero Florian, Hadar Shalev, et al.

Genome Res. published online October 16, 2026
Access the most recent version at doi:10.1101/gr.282119.126

P<P Published online October 16, 2026 in advance of the print journal.

Open Access Freely available online through the *Genome Research* Open Access option.

Creative Commons License This article, published in *Genome Research*, is available under a Creative Commons License (Attribution-NonCommercial 4.0 International), as described at http://creativecommons.org/licenses/by-nc/4.0/.

Email Alerting Service Receive free email alerts when new articles cite this article - sign up in the box at the top right corner of the article or **click here.**



To subscribe to *Genome Research* go to:
https://genome.cshlp.org/subscriptions

© 2026 Gorbonos et al.; Published by Cold Spring Harbor Laboratory Press

Downloaded from genome.cshlp.org on November 17, 2026 . Published by Cold Spring Harbor Laboratory Press

Research

Liver X receptors participate in the fasting response by assisting CEBPB binding to enhancers and promoting the fasting transcriptional program

Tali Gorbonos,[1] Maria C. Romero Florian,[2] Hadar Shalev,[1] Noga Korenfeld,[1] Cigdem Sahin,[2] Sarah A. Shawky,[2] Dana Goldberg,[1] Talia Radushkevitz-Frishman,[1] Mariana Anosov-Babi,[1] Angela Yan,[2] Meital Charni-Natan,[1] Meirav Bar-Shimon,[1] Carolyn L. Cummins,[2] and Ido Goldstein[1]

[1]*Institute of Biochemistry, Food Science and Nutrition, The Robert H. Smith Faculty of Agriculture, Food and Environment, The Hebrew University of Jerusalem, Rehovot 7610001, Israel;* [2]*Department of Pharmaceutical Sciences, Leslie Dan Faculty of Pharmacy, University of Toronto, Toronto, Ontario M5S 3M2, Canada*

Upon fasting, a group of transcription factors (TFs) activates an extensive transcriptional program in the liver to alter hepatocyte metabolism and cope with fasting. This is achieved by TF-mediated activation of enhancers, which become more accessible, leading to gene induction. Nuclear receptor subfamily 1 group H member 3 (NR1H3, also known as liver X receptor-alpha) and 2 (NR1H2, also known as liver X receptor-beta), collectively termed here LXRs, are important TFs known to participate in transcriptional programs in the fed state, but their role in fasting is unclear. Here, we examine the effect of LXR deletion on the transcriptional and chromatin programs activated in the fasted and fed states. We profile the liver transcriptome and genome-wide chromatin accessibility in single-knockout mice lacking either LXR isoform and in double-knockout mice lacking both isoforms. We find that double-knockout of LXRs impairs fasting-induced genes and enhancers. Analysis of genome-wide NR1H3 binding by ChIP-seq, together with chromatin accessibility profiling by ATAC-seq, shows that NR1H3 directly binds enhancers and increases their accessibility. We find that LXRs assist the binding of CCAAT enhancer binding protein beta (CEBPB) to enhancers during fasting. CEBPB is a key TF regulating the fasting response, and its genome-wide binding is perturbed in the absence of LXRs. Cooperation between LXRs and CEBPB promotes fasting-dependent gene induction. These findings reveal a previously unknown role for LXRs in the fasting response, whereby LXRs bind and increase enhancer accessibility, assist CEBPB binding, and promote gene induction. This study demonstrates the complex cooperation of TFs in regulating gene expression to maintain homeostasis during fasting and places LXRs as novel regulators of the fasting response.

[Supplemental material is available for this article.]

In the course of fasting, mammals activate a response aimed to cope with the lack of available energy. A hallmark of the fasting response is the hepatic production of fuels from reservoirs. The liver produces glucose (by glycogenolysis and gluconeogenesis) as well as ketone bodies (by ketogenesis). These fuels are released into circulation and are taken up by other tissues to serve as a source of energy. When food becomes available again, the liver switches from producing fuel to storing energy in the form of glycogen and triglycerides (Secor and Carey 2016; Goldberg and Goldstein 2026).

The liver's metabolic response to fasting is strongly regulated at the transcriptional level. Thousands of genes in hepatocytes are regulated during fasting to accommodate fuel production and limit nonurgent metabolic pathways that demand energy. As such, genes involved in gluconeogenesis, fatty acid oxidation, lipid catabolism, amino acid catabolism, and ketogenesis are induced, whereas genes involved in lipogenesis, glycolysis, and cholesterol synthesis are repressed. This extensive gene expression program is brought about by various transcription factors (TFs) (Goldstein and Hager 2015; Bideyan et al. 2021). Upon fasting, these TFs bind their recognition motifs within enhancers: DNA regulatory regions that serve as a hub for the binding of TFs and other modulators of gene transcription (Gasperini et al. 2020). TF binding to enhancers initiates a chain of events causing enhancer activation and subsequent gene induction. Upon enhancer activation, the chromatin at enhancer regions is decompacted owing to the activity of histone-modifying enzymes and chromatin remodelers (Swinstead et al. 2016b). This enhancer "opening" is crucial for the mutual binding of various TFs as well as transcriptional regulators and is often used as a measurement for enhancer activity levels. Indeed, many hepatic TFs were shown to activate enhancers as measured by increased accessibility (Grøntved et al. 2013; Goldstein et al. 2017a; Quagliarini et al. 2019; Præstholm et al. 2020b; Bideyan et al. 2022; Hunter et al. 2022).

Many TFs regulate fuel production during fasting (Goldstein and Hager 2015). The most well-established TFs shown to play a genome-wide role in fasting are cAMP response element binding

Corresponding authors: ido.goldstein@mail.huji.ac.il, carolyn.cummins@utoronto.ca

Article published online before print. Article, supplemental material, and publication date are at https://www.genome.org/cgi/doi/10.1101/gr.282119.126. Freely available online through the *Genome Research* Open Access option.

© 2026 Gorbonos et al. This article, published in *Genome Research*, is available under a Creative Commons License (Attribution-NonCommercial 4.0 International), as described at http://creativecommons.org/licenses/by-nc/4.0/.

Downloaded from genome.cshlp.org on November 17, 2026 . Published by Cold Spring Harbor Laboratory Press

protein (CREB1), the glucocorticoid receptor (GR; NR3C1), CCAAT enhancer binding protein beta (CEBPB), forkhead box protein O1 (FOXO1), and peroxisome proliferator-activated receptor alpha (PPARA) (Goldstein and Hager 2015; Præstholm et al. 2020a; Fougerat et al. 2024). Studies have shown that the widespread transcriptional program activated during fasting is achieved by cooperation between TFs that work together to induce genes. One of the manners by which TFs cooperate to induce genes is "assisted loading." In assisted loading, one TF binds an enhancer, decompacts chromatin, and partly activates the enhancer (Swinstead et al. 2016b). Increased enhancer accessibility paves the path for a second TF that binds the enhancer, leading to full enhancer activation and maximal gene induction. Assisted loading does not depend on physical interaction between the two TFs. Rather, the first TF indirectly promotes the binding of the second TF by increasing enhancer accessibility. Assisted loading is operative in fasting in which two fasting hormones, glucagon and glucocorticoids, cooperate to synergistically induce genes; glucagon activates CREB1, and glucocorticoids activate NR3C1 (GR). CREB1 assists the loading of NR3C1 in one set of enhancers, whereas NR3C1 assists the loading of CREB1 at another set of enhancers in a manner not necessitating physical interaction between them (Goldstein et al. 2017a; Goldberg et al. 2022). This mutual assisted loading leads to synergistic induction of gluconeogenic genes and augments gluconeogenesis (Goldstein et al. 2017a; Korenfeld et al. 2021; Goldberg et al. 2022). Assisted loading in the liver was also described in nonfasted conditions in which CEBPB assisted the binding of NR3C1 (Grøntved et al. 2013). This finding aligns with the well-established role of CEBPB and its close relative CEBPA as lineage-determining factors that open most hepatic enhancers and facilitate the binding of signal-activated TFs (such as NR3C1) to them (Roesler 2001; Goldstein 2020).

Among the various hepatic TFs regulating metabolic pathways, nuclear receptor subfamily 1 group H (NR1H, also known as liver X receptors [LXRs]) stand out as principal regulators of lipogenesis, cholesterol homeostasis, and bile acid metabolism. Following their activation by cholesterol derivatives, LXRs regulate a wide variety of genes involved in metabolism (Janowski et al. 1996; Calkin and Tontonoz 2012). Hepatocytes express two LXR isoforms: NR1H3 and NR1H2 (Wang and Tontonoz 2018). Some studies show unique roles for each isoform in terms of gene expression and metabolic effects (Peet et al. 1998; Patel et al. 2011, 2017; Heckmann et al. 2017), whereas other studies show compensation between the two isoforms when one is deleted (Quinet et al. 2006; Ramón-Vázquez et al. 2019). LXRs play a major role in the fed state by supporting lipogenic gene expression (Wang and Tontonoz 2018). The role of LXRs in the refeeding period following fasting is even more pronounced; LXRs govern the "fat overshoot" phenomenon in which lipogenesis is rampant and reaches higher levels than prefasting levels (Korenfeld et al. 2024). Although the role of LXRs in fed states is well established, their role in fasting is only sparsely reported; NR1H3 increases the levels of G0S2 during fasting (Heckmann et al. 2017) and promotes glycogen depletion (Oosterveer et al. 2008). NR1H2 was shown to be important for NR3C1-dependent induction of gluconeogenic genes and in glucocorticoid-induced hyperglycemia (Patel et al. 2011, 2017).

Thus, there are a few lines of evidence pointing to a role of LXRs in fasting, but it is not known if LXRs regulate different genes under different nutritional states (fasting, refeeding, etc.) and if they cooperate with other TFs in a manner dependent on the nutritional state. It is also unclear whether the different LXR isoforms separately regulate distinct gene expression programs or whether they completely compensate for each other's activity. We hypothesized that gene regulation by LXRs is tightly linked to the liver's nutritional state. To define isoform-specific roles and cross-isoform compensation, we used LXR single- and double-knockout (KO) mouse models. We utilized transcriptome profiling as well as genome-wide measurements of enhancer accessibility and TF binding to unravel the role of LXRs in different nutritional states.

Results

LXRs extensively alter hepatic gene expression and enhancer accessibility according to the nutritional state

We aimed to examine and compare the effect of LXRs on hepatic gene expression in different nutritional states. We used whole-body *Nr1h3*$^{-/-}$ (αKO) mice, *Nr1h2*$^{-/-}$ (βKO) mice, or dual *Nr1h3*$^{-/-}$ *Nr1h2*$^{-/-}$ (double knockout [DKO]) mice (Fig. 1A; Supplemental Fig. S1A). These mice, together with wild-type (WT) mice were divided into three groups: ad libitum fed mice that had unrestricted access to food (Adlib), mice that did not have access to food for 24 h (Fasted), and mice fasted for 24 h followed by refeeding for another 24 h (Refed) (Fig. 1A). A period of 24 h of fasting was chosen because this length of fasting fully encompasses the metabolic characteristics of the fasting response: glycogen breakdown, gluconeogenesis, and ketogenesis (Cariou et al. 2005; Carper et al. 2020; Defour et al. 2020; Smati et al. 2022). Similarly, 24 h of refeeding are needed to fully activate hepatic lipogenesis and other aspects of the recovery from fasting (Korenfeld et al. 2024).

We used RNA-seq to map the hepatic transcriptome of each nutritional state for the four mouse genotypes. We started by obtaining a general view of the differences in gene expression between groups using dimensionality reduction analysis. As expected, we found that fasting significantly alters the transcriptome, with the Fasted group distinctly separated from the Adlib and Refed groups. The transcriptome of the αKO and βKO mice was similar to that of the WT mice, whereas most DKO mice were separated from the other genotypes in all nutritional states (excluding one mouse in the Fasted DKO group) (Fig. 1B). This suggests that LXR isoforms largely compensate for each other's activity, but when both are missing, gene expression patterns are extensively affected. To precisely evaluate the effect of LXRs on gene expression, we performed a set of pairwise comparisons (Supplemental Fig. S1B). We defined genes as "LXR-increased" if their level was higher in WT compared with KO and as "LXR-decreased" if their level was lower in WT compared with KO. In single-KO mice, we found only several dozens of LXR-regulated genes (i.e., either increased or decreased) across all nutritional states. This aligns with Figure 1B, which shows high similarity between single-KO mice and WT mice. In contrast, each nutritional state showed numerous LXR-regulated genes when comparing WT with DKO mice. This was most evident in the Refed group but was also very dominant in the Fasted and Adlib groups (Fig. 1C; Supplemental Fig. S1B). In total, we found 3322 LXR-regulated genes across nutritional states; that is, genes increased or decreased in the WT compared with at least one KO mouse line: αKO, βKO, or DKO (Supplemental Table S1). Of note, 93.1% of the LXR-regulated genes were not different from the WT in the single-KO mice, suggesting that the LXR isoforms largely compensate for one another when only one isoform is deleted (Supplemental Table S1).

Downloaded from genome.cshlp.org on November 17, 2026 . Published by Cold Spring Harbor Laboratory Press

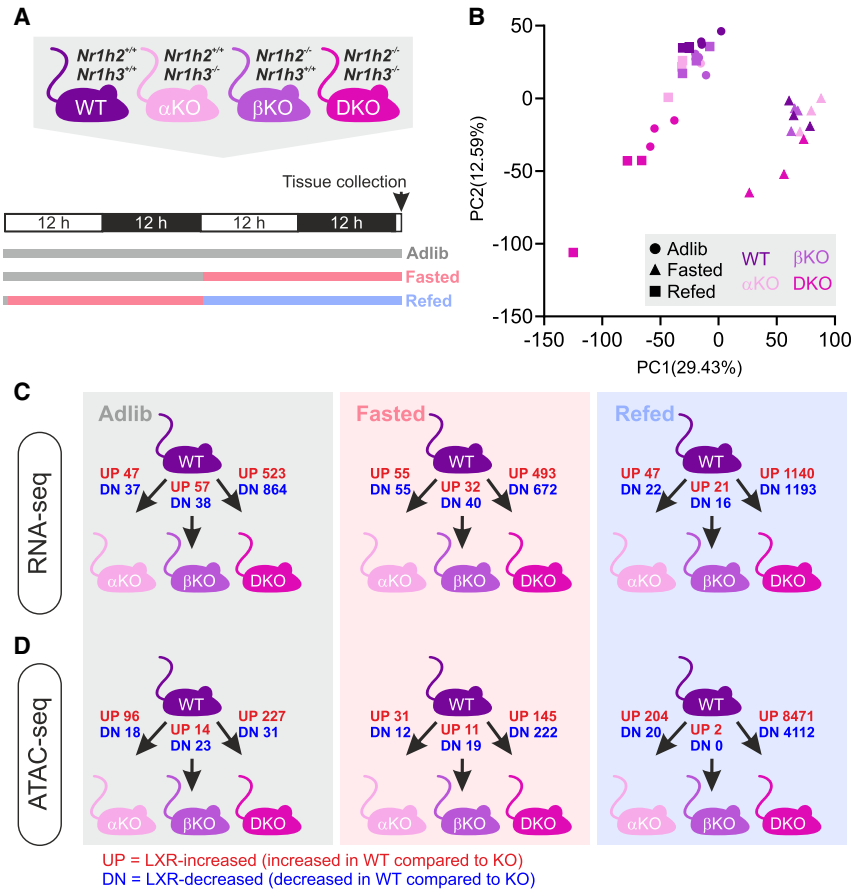


Figure 1. LXR deletion alters gene expression and chromatin accessibility, with the effect varying across nutritional states. (*A*) Experimental design. Mice carrying four genotypes (WT, αKO, βKO, and DKO) were subjected to three nutritional conditions: ad libitum feeding (Adlib), a 24 h fast (Fasted), or a 24 h fast followed by 24 h of refeeding (Refed). All mice were euthanized on the same day, 1 h after lights on. Liver and plasma samples were collected for downstream analyses. (*B*) Gene expression patterns across liver RNA-seq groups were analyzed by principal component analysis (PCA), illustrating that fasting exerts the most widespread effect on gene expression, followed by a double deletion of *Nr1h3* and *Nr1h2*. (*C*,*D*) Pairwise comparisons of differential RNA expression (*C*) and chromatin accessibility (*D*) between livers from WT mice and each single-KO genotype show limited effects. However, DKO alters gene expression and chromatin accessibility in all nutritional states. (UP) LXR-increased (higher in WT compared with KO); (DN) LXR-decreased (lower in WT compared with KO). *D*ifferential gene expression (*C*) and chromatin accessibility (*D*) were determined by DESeq2 (fold change ≥1.5, adjusted *P*-value ≤0.05).

We hypothesized that because LXRs broadly affect gene expression, they may also be involved in enhancer activation, as gene induction and enhancer activation are tightly linked (Gasperini et al. 2020). To explore this possibility, we profiled hepatic chromatin accessibility under the different nutritional states and tested how it is affected by the lack of LXRs. We performed assay for transposase-accessible chromatin sequencing (ATAC-seq) following the same experimental design described in Figure 1A. We found a total of 192,706 accessible sites in the liver across all conditions; 86% of them were located at either intergenic or intronic regions, areas known to harbor enhancers (Supplemental Fig. S2A). These accessible sites were enriched for the HNF4A motif (DR1), a TF known for regulating liver functions and binding most liver enhancers (Supplemental Fig. S2B; Hunter et al. 2022). These sites were also enriched for H3K27 acetylation, a known enhancer mark (Supplemental Fig. S2C). Together, these data suggest that the accessible sites we found are enriched with markers of liver enhancers.

To measure the effect of LXRs on enhancer accessibility, we analyzed LXR-dependent changes in chromatin accessibility by pairwise comparisons of the WT versus each KO mouse. Most differentially accessible sites were found in DKO mice, suggesting substantial compensation between LXR isoforms in regulating enhancer accessibility and aligning with the RNA-seq data (Fig. 1D; Supplemental Table S2). Similar to gene expression, LXRs had the largest effect on the Refed group, but the Fasted and Adlib groups also showed significant alterations in chromatin accessibility (Fig. 1D; Supplemental Table S2). Taken together, these results show that LXRs affect hepatic gene expression and enhancer accessibility. The effect depends on the nutritional state, and most of it is not specific to either of the LXR isoforms.

Lipogenesis-related genes and hepatic triglyceride accumulation are controlled by NR1H3

Although LXR isoforms mostly compensate for each other, our results show some isoform-specific effects. Combining all nutritional states, we found 203 NR1H3-specific genes and 154 NR1H2-specific genes (Supplemental Table S1). Gene Ontology enrichment analysis showed a high enrichment of lipogenic genes among NR1H3-specific increased genes (Supplemental Table S1). Indeed, lipogenic genes, including *Acly*, *Acss2*, and *Elovl6*, showed a clear NR1H3-dependent increase in the Refed state but were unaffected by NR1H2 (Fig. 2A). This is consistent with previous studies showing NR1H3-dependent increase in lipogenic gene expression and NR1H3 binding near lipogenic genes (Peet et al. 1998; Repa et al. 2000; Zhang et al. 2012; Heckmann et al. 2017; Korenfeld et al. 2024). Genes increased in an NR1H2-specific manner were also found (e.g., *Gpcpd1*, *Moxd1*, *Elovl3*) (Fig. 2B), but they did not produce relevant enriched Gene Ontology terms, suggesting there is no apparent pathway regulated exclusively by the NR1H2 isoform (Supplemental Table S1).

Given the NR1H3-specific induction of lipogenic genes, we measured triglyceride levels in plasma and the liver. Liver triglyceride levels were significantly lower in both the Refed αKO and DKO mice, whereas the levels in the Refed WT and βKO mice were indistinguishable from each other (Fig. 2C). This distinction between WT/βKO on the one hand and αKO/DKO on the other hand was observed also in Fasted mice but not in Adlib mice, in which all samples showed similarly low levels of liver triglycerides (Fig. 2C). Plasma triglyceride levels were also significantly lower in the Refed αKO and DKO mice compared with the Refed WT and

Downloaded from genome.cshlp.org on November 17, 2026 . Published by Cold Spring Harbor Laboratory Press

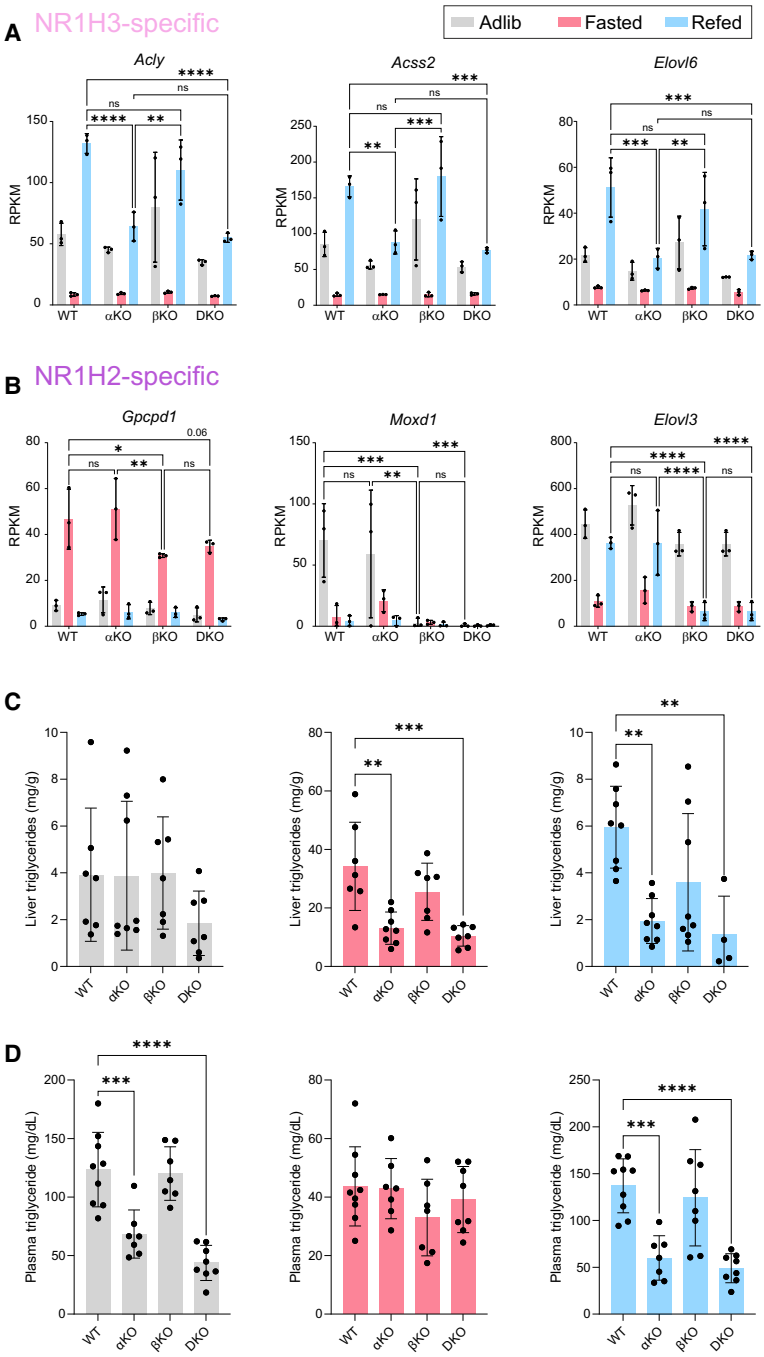


Figure 2. Lipogenesis-related genes and hepatic triglyceride accumulation are controlled by NR1H3. (*A*) Normalized hepatic expression levels of lipogenesis-related genes were measured in the livers of WT, αKO, βKO, and DKO mice across the Adlib, Fasted, and Refed conditions. For all three genes, αKO and DKO mice show similarly reduced expression in Refed mice, whereas βKO mice largely resemble the WT, indicating that NR1H3 is the dominant isoform driving their regulation. (*B*) Normalized hepatic expression levels of *Gpcpd1*, *Moxd1*, and *Elovl3* were measured in the livers of WT, αKO, βKO, and DKO mice across the Adlib, Fasted and Refed conditions. Gene expression levels of these NR1H2-specific genes show similarity in expression between βKO and DKO mice, whereas αKO mice are similar to the WT. (*C*,*D*) Liver (*C*) and plasma (*D*) triglycerides levels were measured in WT, αKO, βKO, and DKO mice in all nutritional states. Because of major differences in the levels of triglycerides between nutritional states, each nutritional state is presented separately to allow genotype-based comparisons rather than fasting-based comparisons. In several nutritional states, triglyceride levels were reduced in αKO and DKO mice, showing that NR1H3 is the major contributor, with no compensation by NR1H2. (*) $P \leq 0.05$, (**) $P \leq 0.01$, (***) $P \leq 0.001$, (****) $P \leq 0.0001$, (ns) $P > 0.05$ by two-way (*A*,*B*) or ordinary one-way (*C*,*D*) ANOVA, post hoc analyses by Holm–Sidak. To improve clarity, only selected statistical tests are shown. (RPKM) Reads per kilobase per million.

βKO mice, which were indistinguishable from each other. This pattern was also observed in the Adlib mice, whereas in the Fasted mice, plasma triglycerides were similarly low across all genotypes (Fig. 2D). We next measured the effect of LXRs on plasma parameters of lipolysis, which are increased during fasting. Plasma free fatty acids were indistinguishable across genotypes in the Adlib and Fasted mice but were lower in the Refed αKO and DKO mice compared with the WT and βKO mice (Supplemental Fig. S1C). Glycerol levels were mostly similar in all genotypes and nutritional states (Supplemental Fig. S1D). Thus, during fasting, LXRs do not affect the products of lipolysis.

Taken together, these results show that LXRs compensate for each other for most of the transcriptional programs governed by them, with the important exclusion of the lipogenesis genes for which NR1H3 is responsible.

LXRs play a specific regulatory role in fasting

After finding that LXRs regulate hundreds of genes in each nutritional state, we asked if LXRs regulate the same genes across all groups or if LXRs regulate different sets of genes depending on the nutritional state. To answer this, we compared LXR-increased genes in each nutritional state: Adlib, Fasted, and Refed. Because of the large degree of mutual compensation by the two isoforms, we focused on the DKO genotype and examined genes that were higher in the WT compared with the DKO. We found considerable differences between nutritional states with LXRs regulating different sets of genes in each state. This was most obvious in Refed, in which 751 genes were increased by LXR only in the Refed condition, but it was also evident in the Fasted state, with 241 genes increased by LXR only in the Fasted group and not in Adlib or Refed (Fig. 3A). These results show that the gene program regulated by LXRs differs significantly as a function of the nutritional state and that LXRs regulate a set of genes only following fasting. This points to a link between LXR-dependent gene regulation and the liver's metabolic status.

Although the role of LXRs in refeeding is well established, their role in fasting is not clear. The finding that LXRs increase the expression of a subset of genes specifically during fasting

Downloaded from genome.cshlp.org on November 17, 2026 . Published by Cold Spring Harbor Laboratory Press

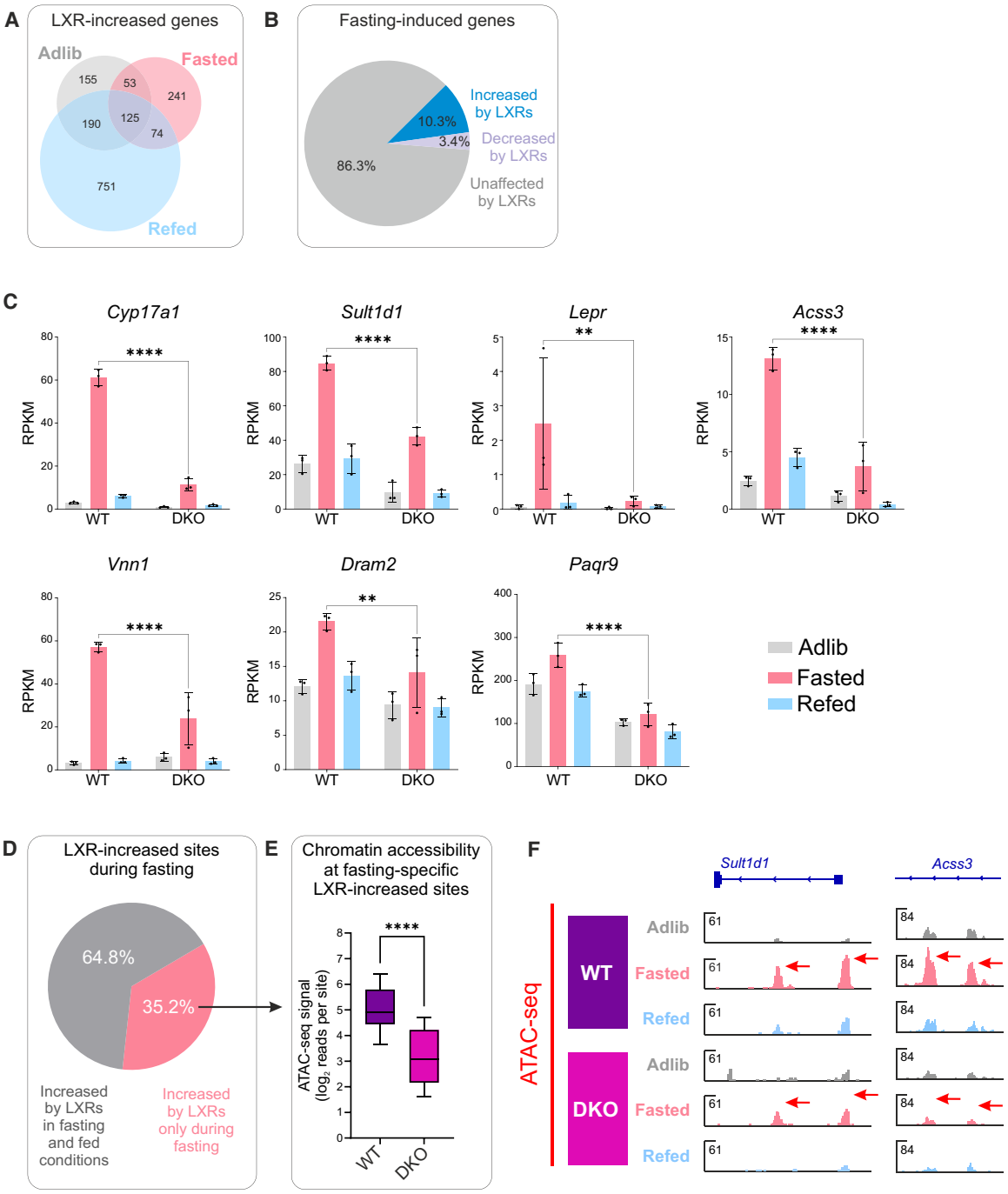


Figure 3. LXRs differentially affect hepatic gene expression and chromatin accessibility depending on the nutritional state, with a unique effect during fasting. (*A*) Liver RNA-seq data for all LXR-increased genes (higher in WT livers compared with DKO) from all nutritional states were compared. The overlap analysis shows that a substantial fraction of LXR-increased genes is unique to each nutritional state. (*B*) Fasting-induced genes (higher in Fasted compared with Refed in the livers of the WT mice) from liver RNA-seq were partitioned based on the effect of LXRs on them (LXR-increased, LXR-decreased, or LXR-unaffected). This revealed that 10.3% of fasting-induced genes are increased by LXRs. (*C*) Normalized gene expression levels are shown in the livers of the WT and DKO mice in the Adlib, Fasted, and Refed states. Fasting-induced, LXR-increased genes reveal a pattern in which the induction of genes during fasting is dependent on LXRs. The fasting-dependent induction of genes is perturbed in LXR DKO. (*D*,*E*) All LXR-increased ATAC sites (higher in the livers of the WT mice compared with the DKO mice) from all nutritional states were compared, showing that LXRs increase enhancer accessibility upon fasting and not only in fed states. Of note, 35.2% of LXR-increased sites are fasting specific and are not elevated in the Refed or Adlib states. Boxplots (*E*) show reduced chromatin accessibility at these fasting-specific sites in DKO compared with the WT. (*F*) Normalized ATAC-seq signal tracks near LXR-increased, fasting-induced genes are shown in the livers of the WT and DKO mice in all nutritional states. This illustrates both fasting-dependent and LXR-dependent increase in enhancer accessibility. (*) $P \leq 0.05$, (**) $P \leq 0.01$, (***) $P \leq 0.001$, (****) $P \leq 0.0001$, (ns) $P > 0.05$ by an ordinary two-way ANOVA, post hoc analyses by Holm–Sidak (*C*) or by a two-tailed, unpaired *t*-test (*E*). To improve clarity, only selected statistical tests are shown. Genes were determined as differentially expressed between two conditions if they passed these DESeq2 cutoffs: fold change ≥1.5, adjusted *P*-value ≤ 0.05. (RPKM) Reads per kilobase per million.

Downloaded from genome.cshlp.org on November 17, 2026 . Published by Cold Spring Harbor Laboratory Press

prompted us to examine whether LXRs contribute to the hepatic transcriptional response to fasting. We identified 819 fasting-induced genes, defined as genes with increased expression in the WT Fasted mice compared with the WT Refed mice (Supplemental Table S3). As expected, pathways enriched among fasting-induced genes were metabolic pathways associated with fasting, such as gluconeogenesis and fatty acid oxidation (Supplemental Table S3). When we overlapped these fasting-induced genes with LXR-increased genes, we found that 10.3% of fasting-induced genes were increased by LXR during fasting (Fig. 3B). In other words, the fasting-dependent induction of these genes was dampened in DKO mice. These results show that one-tenth of the transcriptional response to fasting is LXR dependent. In contrast, only 3.4% of fasting-induced genes were decreased by LXRs (Fig. 3B). Examples of individual fasting-induced genes show this induction is dampened or abolished altogether in the DKO mice (Fig. 3C).

We examined the magnitude of LXRs' impact compared with "classic" fasting TFs in terms of their effect on genes. We analyzed liver transcriptome data from available studies in which fasting TFs were deleted: PPARA, FOXO1, NR3C1, and CREB3L3 (Kalvisa et al. 2018; Régnier et al. 2018; Ruppert et al. 2019; Kitamoto et al. 2021). Similar to our approach for LXRs, we compared the hepatic transcriptome of the TF KO mice to the control mice (WT or floxed) and extracted a list of genes increased by each TF (Supplemental Table S3). Of note, for each TF, the comparison was made in the Fasted condition. We then overlapped these lists with fasting-induced genes found in this study. Fitting with previous studies, PPARA was the dominant TF with 30% of fasting-induced genes also increased by PPARA (Fougerat et al. 2024). Of note, LXRs showed an effect similar to, and even higher than, prominent fasting TFs; FOXO1 increased only 1.2% of fasting-induced genes, and in CREB3L3, the fraction was 3.9%. NR3C1, the well-known fasting TF, increased 13% of fasting-induced genes. Thus, the magnitude of LXRs on fasting-induced genes is comparable, or even higher than, that of TFs with an established role in fasting.

The specific contribution of LXRs to the fasting response was also evident in chromatin accessibility data. Among LXR-increased sites in the Fasted group (shown in Fig. 1D), 35% were increased by LXRs only in the Fasted group and not in the Adlib or Refed groups (Fig. 3D,E). This shows that LXRs specifically increase the accessibility of enhancers in response to fasting. Examples of two loci near LXR-increased fasting-induced genes depict the effect of LXRs on chromatin: Enhancers show increased accessibility specifically upon fasting, but this increase is completely negated in DKO mice (more examples of loci are provided below) (Fig. 3F). Taken together, these results show that LXRs regulate genes in a manner linked to the nutritional state, with enhancers and gene programs governed by LXRs significantly diverging in fasting/feeding. In contrast to the common perception, these findings reveal a significant role for LXRs in increasing the accessibility of enhancers and genes during fasting, not only during feeding.

NR1H3 directly binds and increases accessibility of thousands of hepatic enhancers

It has been reported that many of the effects of LXRs on hepatic gene expression are indirect and are mediated by the induction of *Srebf1*, the gene encoding SREBP-1c, which in turn induces lipogenic genes (Liang et al. 2002; Rong et al. 2017). This is unlikely to be the case in fasting, as LXRs do not induce *Srebf1* during fasting but only in the Refed or Adlib states (Supplemental Fig. S3A). Also, it was recently shown that the role of LXRs in refeeding is largely mediated by direct induction of genes in the liver (Korenfeld et al. 2024). Therefore, we hypothesized that LXRs regulate most LXR-increased genes by directly binding their respective enhancers. To explore this possibility, we performed motif enrichment analysis in the three groups of LXR-increased enhancers (i.e., sites higher in the WT compared with DKO in Adlib, Fasted, and Refed). The full LXR motif (DR4) was the highest enriched motif among the Adlib as well as the Fasted LXR-increased enhancers, suggesting that LXRs directly bind to these enhancers to regulate genes in fasting and not only refeeding. A half-site of the LXR motif was the most enriched motif within the Refed LXR-increased enhancers (Supplemental Fig. S3B).

The enrichment of the LXR motif in the LXR-increased sites suggests that LXRs regulate these regions by directly binding them. To test this, we performed chromatin immunoprecipitation (ChIP) sequencing (ChIP-seq) for NR1H3 (the predominant isoform in liver) under all nutritional states. To validate the antibody specifically detects NR1H3 and not NR1H2, we performed ChIP-PCR on an LXR site bound by both NR1H3 and NR1H2 (Patel et al. 2017). We found significant ChIP signal in the WT and βKO mice but not in the αKO or DKO mice, showing the antibody specifically binds NR1H3 (Supplemental Fig. S4A). We found a total of 3578 NR1H3 binding sites; most were located in intronic, intergenic, and promoter regions (Supplemental Fig. S4B; Supplemental Table S4). The LXR motif was the top-enriched motif within the NR1H3 binding sites, confirming antibody specificity and ChIP quality (Supplemental Fig. S4C). We used the DKO mice as a control for antibody specificity, and indeed, these sites showed no NR1H3 binding in DKO mice (Fig. 4A).

Binding of an activating TF is often accompanied by increased enhancer accessibility. To test this for NR1H3, we measured NR1H3 binding in LXR-regulated enhancers. An association between NR1H3 binding and increased chromatin accessibility would suggest that NR1H3 induces these enhancers. When examining LXR-regulated enhancers (i.e., chromatin sites showing differential chromatin accessibility between the WT and DKO), we found prominent NR1H3 binding at the LXR-increased enhancers but not at the LXR-decreased enhancers in the Fasted group (Fig. 4B; Supplemental Fig. S4D). Moreover, NR1H3 binding was evident even when examining the subset of LXR-increased sites that are specifically increased by fasting and not in feeding states (Fig. 4C). These observations functionally link NR1H3 binding and increased enhancer accessibility in both the fasting and feeding states. As an example, we show the locus of *Cyp17a1* (Fig. 4D), which is an LXR-dependent fasting-induced gene (Fig. 3C). Fasting causes NR1H3 binding to this locus, leading to increases in enhancer accessibility upon fasting. The fasting-induced increase in accessibility is negated altogether in DKO mice.

The mRNA levels of LXRs were unaltered by fasting or refeeding (Supplemental Fig. S1A), excluding the possibility that the effects of LXRs in these states is mediated by transcriptional regulation of their encoding genes. LXRs are activated by derivatives of cholesterol (Janowski et al. 1996). Thus, we examined if hepatic cholesterol levels change following fasting. In both the WT and DKO mice, liver cholesterol was increased by fasting and reduced after refeeding, with a similar trend in the single-KO mice (Supplemental Fig. S4E). This raises the possibility that increased cholesterol levels during fasting promote LXR activation. Collectively, these findings demonstrate that LXRs bind to enhancers specifically during fasting, increase their accessibility, and induce the expression of genes.

Downloaded from genome.cshlp.org on November 17, 2026 . Published by Cold Spring Harbor Laboratory Press

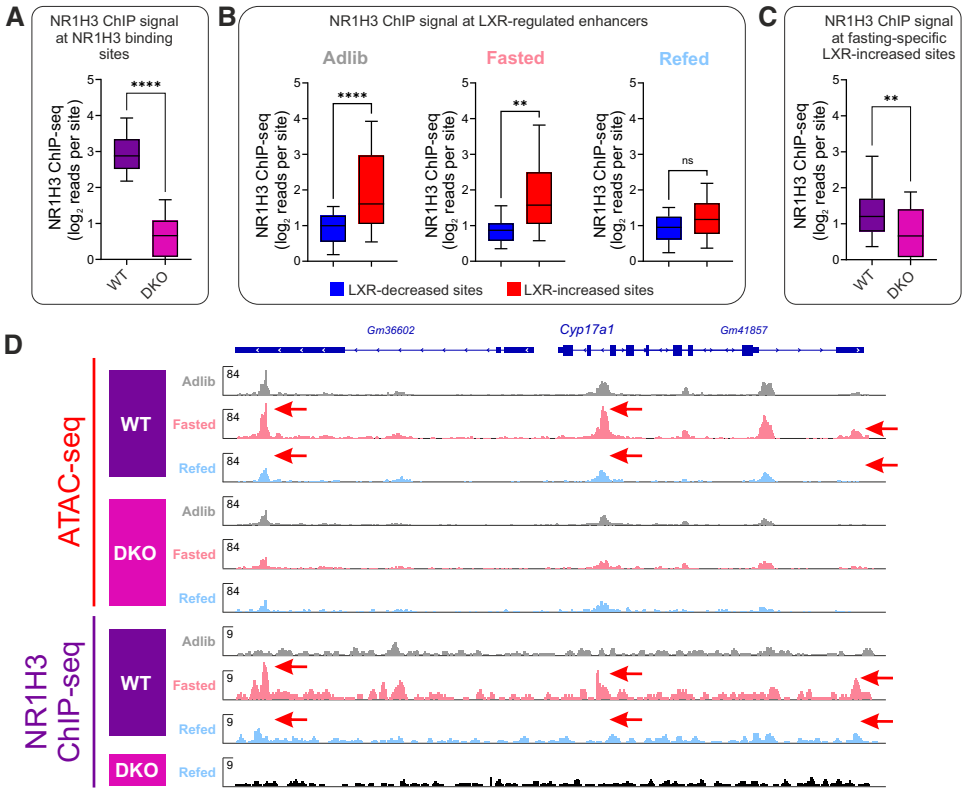


Figure 4. Fasting promotes NR1H3 binding to enhancers with increased accessibility upon fasting. (*A*) NR1H3 ChIP-seq signal was quantified in the livers of the WT and DKO mice across all NR1H3 binding sites, showing that the ChIP-seq signal is derived from bona fide binding of NR1H3, as it is absent in DKO mice. (*B*) NR1H3 ChIP-seq signal was quantified in the livers of WT and DKO mice in all LXR-regulated sites across all nutritional states. Upon fasting, NR1H3 preferentially binds the LXR-increased sites (sites showing higher chromatin accessibility in the WT mice compared with the DKO mice) but not the LXR-decreased sites. (*C*) NR1H3 ChIP-seq signal was quantified in the livers of the WT and DKO mice in fasting-specific, LXR-increased sites (sites with higher chromatin accessibility in the WT mice compared with the DKO mice only in the Fasted condition). This showed NR1H3 binding in fasting-specific LXR-increased sites, suggesting direct induction of LXR-increased enhancers during fasting by NR1H3 binding. (*D*) Normalized ATAC-seq signal and NR1H3 ChIP-seq signal tracks near *Cyp17a1*, an LXR-increased, fasting-induced gene, are shown in the livers of the WT and DKO mice in the Adlib, Fasted, and Refed states. This reveals a fasting-dependent and LXR-dependent increase in enhancer accessibility as well as fasting-induced binding of NR1H3. (*) $P \leq 0.05$, (**) $P \leq 0.01$, (***) $P \leq 0.001$, (****) $P \leq 0.0001$, (ns) $P > 0.05$ by a two-tailed, unpaired *t*-test (*A*,*C*) or by ordinary one-way ANOVA, post hoc analyses by Holm–Sidak (*B*).

LXRs assist the loading of CEBPB on fasting enhancers

The transcriptional response to fasting is complex and includes various TFs that often cooperate to induce genes during fasting. We hypothesized that LXRs are no exception and that they cooperate with other TFs to induce genes during fasting. This hypothesis is plausible because LXRs participate in both the fed and fasted states. Therefore, to produce a response tailored to each nutritional status, it is probable that LXRs cooperate with different TFs governing the transcriptional program of each state. To explore possible cooperation between LXRs and other TFs, we examined the motifs enriched at LXR binding sites under the assumption that motifs for TFs cooperating with LXRs will be enriched. Among the top motifs enriched at LXR binding sites, we found the DR4 LXR motif as well as the similar DR1 nuclear receptor motif and nuclear receptor half sites. The DR1 motif is bound by PPARA, and its enrichment in LXR-increased sites is consistent with previous observations of cooperation between NR1H3 and PPARA (Boergesen et al. 2012). PPARA is a prominent fasting TF with well-established roles in the hepatic fasting response (Kersten 2014). To relate the DR1 motif enrichment with actual PPARA binding, we analyzed available PPARA ChIP-seq in livers of fasted mice (Sommars et al. 2019) and overlapped PPARA binding sites with LXR-increased sites during fasting. We found that 57% of the LXR-increased sites are bound by PPARA. We performed a similar analysis with other prominent fasting TFs profiled by ChIP-seq in the livers of fasted mice: NR3C1, CREB1, and FOXO1 (Goldstein et al. 2017a; Kalvisa et al. 2018). In contrast to the substantial overlap observed in PPARA, other fasting TFs showed negligible binding in LXR-increased sites (6%, 7%, and 6%, respectively). These results suggest that the previously reported cross talk between PPARA and LXR may partake in the hepatic response to fasting.

Among motifs enriched in LXR-increased sites, only one top-enriched motif was not a nuclear receptor motif and was therefore an interesting outlier: the CEBP motif (Supplemental Fig. S4C). CEBPB is a liver-predominant member of the CEBP family and is well known to regulate gene expression during fasting (Roesler 2001; Goldberg et al. 2024). Therefore, we surmised it may cooperate with LXRs in regulating fasting-dependent gene induction. We performed ChIP-seq for CEBPB in the WT and LXR DKO mice under all nutritional states. We identified a total of 32,562 CEBPB sites, most of which were located in intronic, intergenic, and promoter regions (Supplemental Fig. S5A; Supplemental Table S4). As expected, the CEBP motif was enriched in CEBPB binding sites, confirming antibody specificity (Supplemental Fig. S5B). CEBPB

Downloaded from genome.cshlp.org on November 17, 2026 . Published by Cold Spring Harbor Laboratory Press

binding was increased upon fasting, with 8639 CEBPB binding sites found only in the Fasted group (Fig. 5A). In the Fasted state, CEBPB binding was reduced in the DKO mice; the WT mice had 11,985 sites that were not detected in the DKO mice (Fig. 5B). This shows that CEBPB binding is significantly reduced in DKO, in many cases below the peak-calling threshold, resulting in fewer binding events detected and the loss of 60% of sites. LXRs also affected CEBPB binding in the refed state, in which 8101 binding sites were only detected in the WT mice (Supplemental Fig. S5C).

Although LXRs affect CEBPB binding in both the fasted and refed states, we focused on the fasted state for several reasons: CEBPB has principal roles in the fasting response (Liu et al. 1999; Goldstein and Hager 2015; Goldberg et al. 2024); the number of CEBPB sites is significantly increased upon fasting (Fig. 5A), suggesting increased activity; and the effect of LXRs on CEBPB binding spans almost 4000 more binding sites in the Fasted mice than in the Refed mice (Fig. 5B; Supplemental Fig. S5C). To interrogate LXR–CEBPB cross talk on fasting-relevant sites, we next focused only on genomic sites with increased accessibility upon fasting. We determined 4540 such sites (higher in the WT Fasted compared with the WT Refed) (Supplemental Table S3). Measuring CEBPB binding levels within these sites showed increased binding following fasting compared with the Refed state. This reinforces previous findings of the important role of CEBPB in the fasting response (Roesler 2001; Goldstein et al. 2017a; Goldberg et al. 2024). The fasting-dependent increase in CEBPB binding was completely negated in the DKO mice. In these mice, fasting was unable to augment CEBPB binding (Fig. 5C). Thus, CEBPB binding increases upon fasting with the help of LXRs. In the absence of LXRs, CEBPB binding is significantly perturbed, and fasting is unable to augment it. To further emphasize the link between fasting, LXR, and CEBPB, we focused on sites increased by LXRs only in fasting and not in other nutritional states. Indeed, CEBPB bound these sites in the WT mice, but its binding was perturbed in the DKO mice (Supplemental Fig. S6A). This links LXR-mediated increase in chromatin accessibility during fasting and fasting-induced binding of CEBPB. We show some genomic loci as examples (Fig. 5D; Supplemental Fig. S6B). NR1H3 binds to these loci following fasting, and chromatin accessibility increases during fasting; however, this is negated altogether in the DKO mice. CEBPB binding also increases after fasting, and this increase is perturbed in the DKO mice.

When measuring the distance between CEBP and LXR motifs within enhancers, we found no fixed spacer length between them, and the distances spanned hundreds of nucleotides (Supplemental Fig. S6C). This is at odds with a model whereby LXRs and CEBPB heterodimerize and together bind a composite motif. Therefore, this result suggests that the LXR–CEBPB cooperation does not require protein–protein interaction between the two TFs. Furthermore, deletion of LXRs did not affect total RNA levels of CEBPB, showing that LXRs do not promote CEBPB activity by increasing its expression (Supplemental Fig. S6D).

Collectively, these findings show that during fasting, LXRs assist the loading of CEBPB on enhancers near fasting-induced genes, whereby LXRs increase enhancer accessibility, creating an environment more amenable to CEBPB binding. The effect of LXRs on CEBPB is surprising considering that CEBPB is classically considered a TF whose role is to facilitate the binding of other TFs and not vice versa.

LXRs and CEBPB support gene induction by fasting hormones

Our findings show a cooperation between LXRs and CEBPB occurring during fasting, aligning with the role of LXRs in regulating

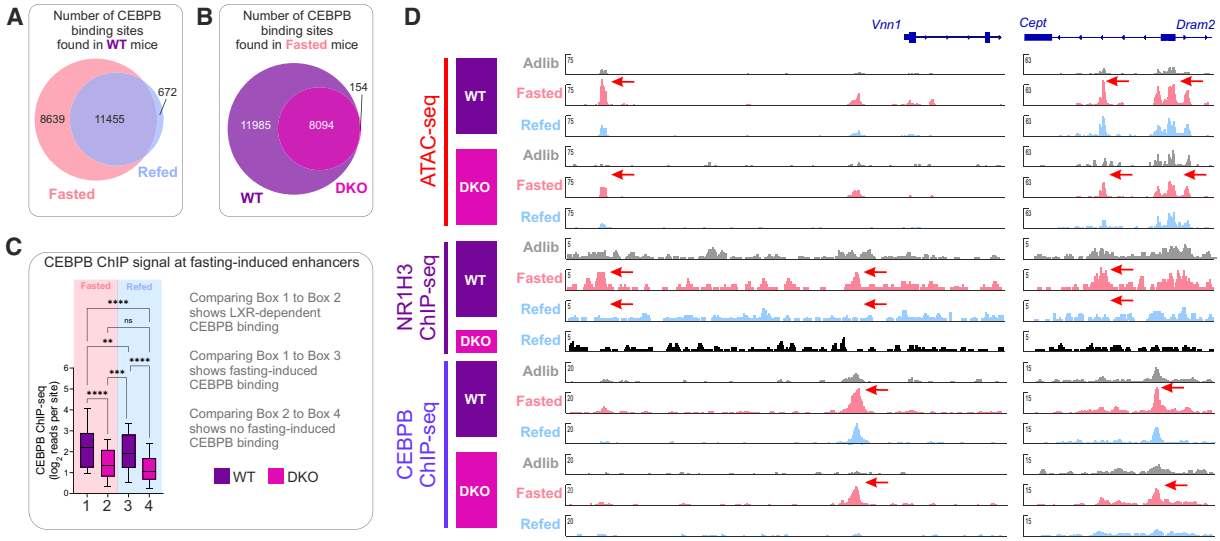


Figure 5. LXRs assist the loading of CEBPB on enhancers with increased accessibility upon fasting. (*A*) CEBPB ChIP-seq was performed, and the number and genomic positions of CEBPB binding sites found in the Fasted and Refed conditions were compared in the livers of the WT mice, revealing that fasting potently induces CEBPB binding in thousands of genomic regions. (*B*) The number and genomic positions of CEBPB binding sites found in the livers of the WT and DKO mice were compared by CEBPB ChIP-seq in the Fasted state, revealing that LXR deletion abrogates CEBPB binding in thousands of genomic regions during fasting. (*C*) CEBPB ChIP-seq signal was quantified in the livers of the WT and DKO mice across all enhancers with increased accessibility upon fasting, showing induction of CEBPB binding upon fasting (cf. box 1 and box 3). CEBPB binding was perturbed in DKO mice (cf. box 1 and box 2). Contrary to the WT mice, in the DKO mice fasting was unable to increase CEBPB binding (cf. box 2 and box 4). Thus, LXR deletion perturbs fasting-induced CEBPB binding. (*D*) Normalized ATAC-seq, NR1H3 ChIP-seq, and CEBPB ChIP-seq tracks are shown in the livers of the WT and DKO mice in the Adlib, Fasted, and Refed states. This reveals a fasting-dependent and LXR-dependent increase in enhancer accessibility as well as fasting-induced binding of NR1H3 and CEBPB. The binding of CEBPB was perturbed in DKO mice. (*) $P \leq 0.05$, (**) $P \leq 0.01$, (***) $P \leq 0.001$, (****) $P \leq 0.0001$, (ns) $P > 0.05$ by ordinary one-way ANOVA, post hoc analyses by Holm–Sidak.

Downloaded from genome.cshlp.org on November 17, 2026 . Published by Cold Spring Harbor Laboratory Press

fasting-induced genes (Figs. 3–5). CEBPB was recently shown to augment and amplify gene induction caused by the fasting hormones glucagon and glucocorticoids (Goldberg et al. 2024). Therefore, we hypothesized that LXRs increase gene expression during fasting by cooperating with CEBPB, thereby optimizing the response to fasting hormones. To test this, we examined the expression of two LXR-increased, fasting-induced genes, *Sult1d1* and *Lepr*. In hepatocytes, *Sult1d1* is induced by glucocorticoids, and *Lepr* is induced by glucagon (Wong et al. 2010; Nason et al. 2020; Goldberg et al. 2022). We treated primary mouse hepatocytes with corticosterone (the major mouse glucocorticoid), leading to *Sult1d1* induction. This induction was dependent on the glucocorticoid receptor NR3C1 as it was abolished in the presence of RU486, a NR3C1 antagonist (Fig. 6A). To test if *Sult1d1* induction by corticosterone requires CEBPB, we treated hepatocytes with short hairpin RNA (shRNA) against CEBPB prior to corticosterone stimulation. The efficiency of CEBPB knockdown by shRNA was 90% (Supplemental Fig. S6E). The induction of *Sult1d1* by corticosterone was dampened when CEBPB expression was perturbed (Fig. 6B). To test if *Sult1d1* induction is dependent on LXRs also in primary hepatocytes and not only in the liver, we treated hepatocytes with corticosterone together with either an LXR agonist (GW3965) or an antagonist (GSK2033). The corticosterone-dependent induction of *Sult1d1* was augmented in the presence of GW3965 but perturbed in the presence of GSK2033 (Fig. 6C). We next tested corticosterone-dependent induction of *Sult1d1* in two models of LXR gene perturbation. In the first, primary mouse hepatocytes were transfected with small interfering RNAs (siRNAs) targeting both LXR isoforms, leading to a robust decrease in their expression (Supplemental Fig. S6F). In the second model, we used $Nr1h3^{fl/fl}$ and $Nr1h2^{fl/fl}$ double-floxed mice. These mice were injected with hepatocyte-targeted AAV-Cre to induce deletion of both LXR isoforms in hepatocytes, with AAV-GFP used as the control (Supplemental Fig. S6G). Primary mouse hepatocytes were subsequently isolated from these mice 16 days later and treated with corticosterone. *Sult1d1* levels were not affected by LXR perturbation in both the siRNA and gene KO models (Fig. 6D,E). Together, these data suggest that *Sult1d1* is induced by corticosterone in a manner requiring NR3C1 and CEBPB. The reliance on LXRs is only observed in agonist/antagonist experiments but not in the gene perturbation models.

To test *Lepr* regulation, we treated primary mouse hepatocytes with glucagon, leading to *Lepr* induction. Most glucagon-dependent gene induction is mediated by CREB1 (Goldstein and Hager 2018). Indeed, the induction of *Lepr* by glucagon was abolished when CREB1 was inactivated by a dominant-negative peptide (Fig. 6F). *Lepr* induction by glucagon was fully dependent on CEBPB, as no induction was observed when CEBPB expression was perturbed (Fig. 6G). Similarly to *Sult1d1*, *Lepr* was also regulated by LXR, with GW3965 augmenting the effect of glucagon and GSK2033 dampening it (Fig. 6H). When examining *Lepr* expression following LXR gene perturbation, we found that both siRNA-mediated depletion and gene KO impaired glucagon-dependent induction of *Lepr* (Fig. 6I,J). Thus, *Lepr* is induced by glucagon in a manner requiring three TFs: CREB1, CEBPB, and LXRs. Consistent with these observations, we found that NR1H3 binds to the *Lepr* locus primarily during fasting, as does CEBPB. Enhancer accessibility is increased in the presence of LXRs, and CEBPB binding is perturbed in DKO mice (Fig. 6K). Collectively, these findings show that LXRs and CEBPB support gene regulation governed by fasting hormones, and this is achieved autonomously in hepatocytes.

Discussion

In this study, we found that LXRs alter enhancer accessibility and gene expression in a manner highly dependent on the nutritional state. Our results show that one-tenth of fasting-induced genes are induced by LXRs. Considering that dozens of TFs are part of the fasting response, this fraction of genes is considerable, and the effect of LXRs on gene expression is similar to that of the classic fasting TF NR3C1. LXRs increase enhancer accessibility during fasting, thereby assisting the loading of CEBPB to fasting enhancers, and the two TFs induce genes during fasting (Fig. 7). LXRs broadly affect liver enhancers in a manner dependent on the nutritional state. A single deletion of one LXR isoform affects gene expression and enhancer accessibility much less than a dual deletion of both isoforms, showing the large degree of compensation between LXR isoforms.

Compensation between the two LXR isoforms was reported under specific contexts (Quinet et al. 2006; Korach-André et al. 2010; Heckmann et al. 2017). However, a transcriptome-wide view of the liver was not performed, and isoform compensation at the chromatin level was never examined. We found here that when one LXR isoform is lacking, the other isoform assumes most of the transcriptional responsibilities. As a result, loss of a single LXR isoform leads to only focused changes in gene expression. One important exception is lipogenic gene expression and hepatic triglyceride accumulation, which is controlled by NR1H3, as we show here and as was previously reported (Peet et al. 1998; Repa et al. 2000; Zhang et al. 2012; Heckmann et al. 2017; Patel et al. 2017). Another important NR1H3-specific role was previously described: the NR1H3-G0S2 axis. This axis is activated during fasting, whereby NR1H3 induces the expression of G0S2, an inhibitor of lipolysis. This increase in G0S2 contributes to hepatic triglyceride accumulation during fasting (Heckmann et al. 2017). This aligns with our observation that liver triglycerides are reduced in αKO mice and DKO mice not only in the refed state but also in the fasted state. The reason for lack of compensation by NR1H2 only in a subset of genes is unclear. Specificity could arise from isoform-selective post-translational modifications, including phosphorylation (Voisin et al. 2020) and *O*-GlcNAcylation (Anthonisen et al. 2010), or from differences in coregulator recruitment (Torra et al. 2008). The NR1H3-specific induction of lipogenic genes may therefore arise from these isoform-specific effects.

The case of LXRs is unique because they play important roles in both the feeding and fasting response. LXR-directed transcription is dependent on the nutritional state, and LXRs regulate distinct sets of genes in each state. LXRs have a well-documented role in activating gene programs that support metabolic pathways in the fed state (Wang and Tontonoz 2018; Korenfeld et al. 2024). However, their role in fasting was mostly obscure until now. We show that LXRs are responsible for the fasting-dependent induction of 10% of fasting-induced genes. This positions LXRs as important TFs regulating metabolism in both feeding and fasting states.

In the fed state, LXRs increase gene expression both by directly binding to relevant enhancers and inducing genes (Korenfeld et al. 2024) as well as indirectly by increasing the levels of *Srebf1*, encoding the lipogenic TF SREBP-1c (Liang et al. 2002; Rong et al. 2017). Here, we demonstrate that during fasting, LXRs also bind to fasting-specific enhancers, increase their accessibility, and induce the expression of target genes. LXR-mediated increase in enhancer accessibility assists the binding of CEBPB. CEBPB is a key fasting TF responsible for regulating many

Downloaded from genome.cshlp.org on November 17, 2026 . Published by Cold Spring Harbor Laboratory Press

fasting-induced genes and supporting gluconeogenesis (Liu et al. 1999; Goldstein and Hager 2015; Goldberg et al. 2024). We demonstrate here that LXRs and CEBPB cooperate on a genomic scale, in which LXRs assist the loading of CEBPB onto thousands of enhancers to promote the induction of genes during fasting. LXRs bind to enhancers following fasting, increasing their accessibility and thereby promoting CEBPB binding to them. In line with LXR–CEBPB-assisted loading, a recent study found that in immune

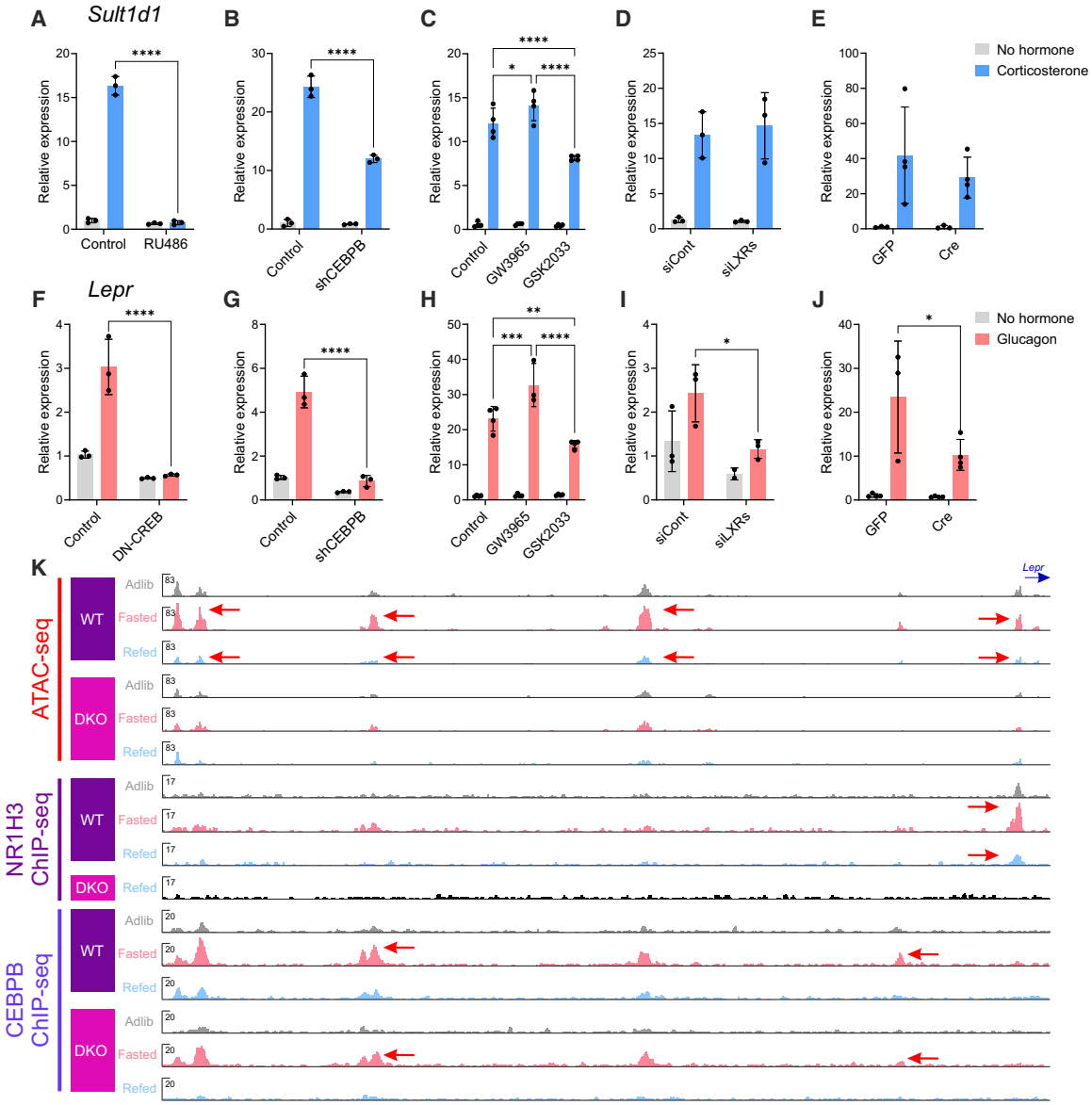


Figure 6. LXRs and CEBPB mediate fasting hormone-controlled gene induction. Primary hepatocytes isolated from WT mice (*A–D*,*F–I*) or *Nr1h3*$^{fl/fl}$, *Nr1h2*$^{fl/fl}$ mice injected with either AAV-Cre or AAV-GFP (*E*,*J*) were treated with 1 µM corticosterone (*A–E*) or 100 nM glucagon (*F–J*) for 8 h prior to harvesting RNA for qPCR analysis. (*A*,*B*) *Sult1d1* expression was increased by corticosterone but suppressed by coaddition of 2 µM RU486 (*A*), and knockdown of CEBPB by shRNA (shCEBPB) added 16 h before corticosterone was added (*B*). (*C*) Corticosterone-mediated increased *Sult1d1* expression was further increased by cotreatment with an LXR agonist (1 µM GW3965) or decreased with cotreatment of an LXR antagonist (10 µM GSK2033). (*D*) Corticosterone-mediated induction of *Sult1d1* was unaffected by siRNA targeting *Nr1h3* and *Nr1h2*. (*E*) Corticosterone-mediated induction of *Sult1d1* was unaffected by gene deletion of *Nr1h3* and *Nr1h2* (gene expression normalized to *Rplp0*). (*F*) *Lepr* expression was increased after glucagon treatment, but this was abolished when CREB1 was inactivated in the presence of a dominant-negative peptide inactivating CREB1 (DN-CREB, added 16 h before glucagon was added). (*G*) Glucagon-dependent induction of *Lepr* was suppressed in primary mouse hepatocytes that had been treated with shRNA targeting CEBPB (shCEBPB) 16 h before compound addition. (*H*) Glucagon-mediated increased *Lepr* expression was further increased by cotreatment with an LXR agonist (1 µM GW3965) or decreased with cotreatment of an LXR antagonist (10 µM GSK2033). (*I*) Glucagon-mediated induction of *Lepr* was perturbed by siRNA targeting *Nr1h3* and *Nr1h2*. (*J*) Glucagon-mediated induction of *Lepr* was perturbed by gene deletion of *Nr1h3* and *Nr1h2* (gene expression normalized to *Rplp0*). (*K*) Normalized ATAC-seq, NR1H3 ChIP-seq, and CEBPB ChIP-seq tracks near *Lepr*, an LXR-increased, fasting-induced gene are shown in the livers of WT and DKO mice in the Adlib, Fasted, and Refed states. This reveals fasting-dependent and LXR-dependent increases in enhancer accessibility as well as fasting-induced binding of NR1H3 and CEBPB. The binding of CEBPB was perturbed in the DKO mice. (*) $P \leq 0.05$, (**) $P \leq 0.01$, (***) $P \leq 0.001$, (****) $P \leq 0.0001$, (ns) $P > 0.05$ by ordinary one-way ANOVA, post hoc analyses by Holm–Sidak. To improve clarity, only selected statistical tests are shown. (sh) Short hairpin, (si) small interfering, and (DN) dominant negative.

Downloaded from genome.cshlp.org on November 17, 2026 . Published by Cold Spring Harbor Laboratory Press

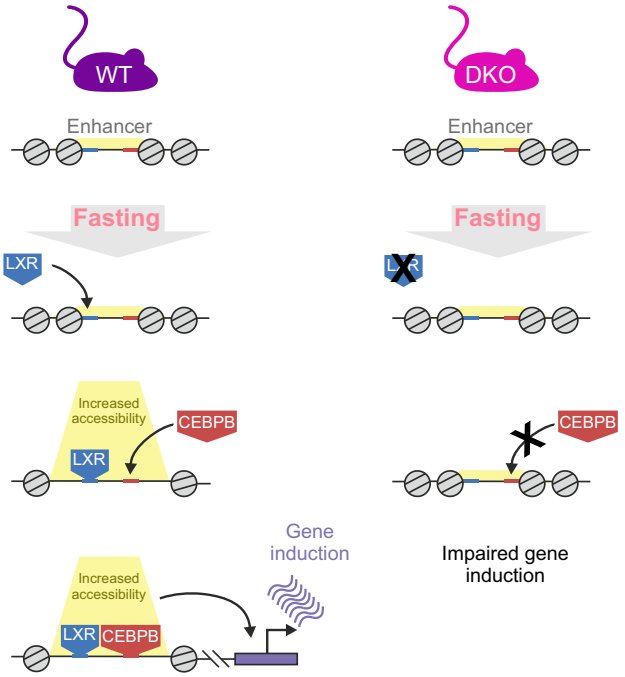


Figure 7. A model for fasting-induced assisted loading of CEBPB by LXRs. Upon fasting, LXRs bind enhancers in the liver, thereby promoting an increase in chromatin accessibility. This altered enhancer environment mediates the binding of CEBPB. The assisted loading of CEBPB by LXRs facilitates gene induction during fasting. In DKO mice, LXRs do not increase enhancer accessibility, thereby precluding CEBPB binding and gene induction.

cells, LXRs and CEBPB cooperate in inducing the *Cd38* gene (Glaría et al. 2025). Cooperation between LXRs and CEBPB is not restricted to fasting. We found that LXRs promote CEBPB binding also upon refeeding, albeit in fewer genomic regions. Our findings align with previous studies: NR1H3 and CEBPB were reported to coregulate the lipogenic gene *Srebf1* in feeding (Tian et al. 2016), and CEBPB deletion prevented LXR-induced accumulation of triglycerides in the liver (Rahman et al. 2013). Considering that LXR promotes hepatic triglyceride accumulation upon refeeding (Korenfeld et al. 2024), our data may provide a mechanistic link between LXR–CEBPB cross talk in refeeding and triglyceride accumulation in the liver.

The role of LXRs in promoting CEBPB binding challenges the common perception of lineage-determining factors and pioneer factors. These types of TFs are responsible for opening chromatin at enhancer regions, thereby facilitating the binding of signal-activated TFs (Heinz et al. 2015; Barral and Zaret 2024). Indeed, CEBPB is considered a lineage-determining factor that assists the binding of NR3C1 at many hepatic enhancers (Grøntved et al. 2013). We show here that assisted loading is bidirectional and that CEBPB needs assistance from LXRs to optimally bind enhancers. This aligns with previous findings showing that the binding of pioneer factors is assisted by other TFs (Swinstead et al. 2016a,b; Seuter et al. 2017; Xu et al. 2024). Our observations, combined with previous studies, highlight that the ability to promote binding of other TFs to enhancers is not unique to pioneer factors; various nonpioneer TFs can also assist the binding of other factors in an enhancer-specific manner (Biddie et al. 2011; Grøntved et al. 2013; Madsen et al. 2014; Goldstein et al. 2017a,b; Goldberg et al. 2022; Lee et al. 2024; Hiltunen et al. 2025). This stems from the common trait shared by most TFs: the ability to recruit coactivators, histone-modifying enzymes, chromatin remodelers, and other factors involved in enhancer activation (Gasperini et al. 2020).

In summary, our findings reveal a substantial role of LXRs in the hepatic transcriptional response to fasting. LXRs promote the increased accessibility of enhancers and the induction of gene expression during fasting. LXRs also potentiate the binding of CEBPB, a key fasting-responsive TF (Fig. 7). These results highlight the complexity of transcriptional regulation during fasting, including cross talk between TFs on the chromatin fiber. Also, we uncover that LXRs take a "double shift" in regulating both fasting and feeding gene programs.

Methods

Animals

WT or whole-body LXR KO mice (*Nr1h3*$^{-/-}$ [αKO], *Nr1h2*$^{-/-}$ (βKO), and *Nr1h3*$^{-/-}$, *Nr1h2*$^{-/-}$ [DKO]) on a C57BL/6 background (a gift from Dr. David J. Mangelsdorf, UT Southwestern) were bred in-house. Male, 8- to 12-week-old mice were placed into one of three groups: Adlib, unrestricted access to a standard rodent chow diet (Teklad 2016S); Fasted, no access to food for 24 h with full access to water; and Refed, fasted for 24 h followed by a refeeding period of 24 h. Food was removed at the beginning of the inactive phase, 1 h after the lights were turned on in the animal facility (Zeitgeber Time 1). The 24 h fasting and refeeding periods help to neutralize circadian clock effects because all samples are collected at the same time of day. Mice were humanely euthanized by decapitation at Zeitgeber Time 1. For hepatocyte-specific deletion of LXRs, mice carrying floxed alleles of both *Nr1h3*$^{fl/fl}$ and *Nr1h2*$^{fl/fl}$ on a C57BL/6 background (gift from Dr. David J. Mangelsdorf) were used. Mice received 1×10^{11} genome copies (GCs) per mouse of AAV.TBG.PI.Cre.rBG (AAV8; Addgene viral prep 107787-AAV8) to induce Cre-mediated deletion of both LXR isoforms in hepatocytes. Control mice received an equivalent dose of AAV.TBG.PI.eGFP.WPRE.bGH (AAV8; Addgene viral prep 105535-AAV8). Primary mouse hepatocytes were subsequently isolated from these mice 16 days later for ex vivo experiments. All animal procedures were conducted in accordance with the standards for the care and use of laboratory animals. The research has been approved by the Faculty of Medicine and Pharmacy Advisory Committee on Animal Care at the University of Toronto; ethics approval number 20012519 (Toronto, Ontario, Canada).

RNA preparation, reverse transcription, and quantitative PCR

Total RNA was isolated from liver pieces (30 mg) or primary hepatocytes using a NucleoSpin kit (Macherey-Nagel 740955) according to the manufacturer's protocol. For quantitative PCR (qPCR), 1 µg of total RNA was reverse-transcribed to generate cDNA (Quantabio 76047-074). qPCR was performed using CFX96 or CFX Opus 384 thermal cycler instruments (Bio-Rad) using SYBR green (Quantabio 101414-276). Gene values were normalized to the housekeeping gene *Rpl13* or *Rplp0* (where indicated). The sequences of primers used in this study are as follows:

Rpl13—Fwd: AGCCTACCAGAAAGTTTGCTTAC; Rev: GCTTCTT CTTCCGATAGTGCATC.

Rplp0—Fwd: CGTCCTCGTTGGAGTGACA; Rev: CGGTGCGTCA GGGATTG.

Downloaded from genome.cshlp.org on November 17, 2026 . Published by Cold Spring Harbor Laboratory Press

Nr1h3—Fwd: GATTAGGGTGGGGGTGACTG; Rev: CTGGAGCC CTGGACATTACC.
Nr1h2—Fwd: GTCCAGCTCTGCCTACATCG; Rev: TTGTAGTGG AAGCCCGAAGC.
Cebpb—Fwd: ATCCGGATCAAACGTGGCTG; Rev: GGCCCGGC TGACAGTTAC.
Sult1d1—Fwd: TGAGCATTGGTCCCAAGTAGAG; Rev: AACTCAG CTTAGGCTGGACAAA.
Lepr—Fwd: TGACTTGCAGATGGTCACCC; Rev: GCAGTTTTTG GGCTCAGACG.

Analysis of liver cholesterol, plasma, and liver triglycerides

Blood was collected into EDTA-containing tubes and centrifuged at 500*g* for 20 min at 4°C to separate the plasma. Plasma triglycerides were measured by an enzymatic colorimetric assay (L-type triglyceride; Fujifilm Wako 992-02892, 998-02992, and 464-01601). Liver samples were cut into pieces (~100 mg each), frozen in liquid nitrogen, and then stored at −80°C until extraction. Lipids were extracted from the liver in chloroform/methanol (2:1, v/v) using the Folch separation technique (Folch et al. 1957). Liver homogenates were then washed with 50 mM NaCl and centrifuged at 1500*g* for 30 min to separate the organic phase, which contained the lipids. Subsequent transfer and washing of organic phases in 0.36 M $CaCl_2$/methanol were performed, followed by centrifugation at 1500*g* for 10 min. Afterward, the organic phases were brought to 5 mL with chloroform in a volumetric flask. Dried aliquots of standards and samples were redissolved in 10 µL of 1:1 chloroform/Triton X-100 overnight and assayed the following day for triglycerides using Infinity triglyceride reagent (Thermo Fisher Scientific TR22421) and cholesterol (Infinity, Thermo Fisher Scientific).

Chromatin immunoprecipitation

ChIP was performed as previously described (Sommars et al. 2019) with modifications: Liver pieces (150 mg) were cross-linked with phosphate-buffered saline (PBS) containing 2 mM disuccinimidyl glutarate (DSG; Santa Cruz Biotechnology sc-285455). Livers were homogenized with a Dounce homogenizer and rotated for 30 min at room temperature. Samples were centrifuged, and the pellet was resuspended with PBS containing 1% formaldehyde (Electron Microscopy Sciences 15714) for further cross-linking. After 10 min, samples were quenched with 0.125 M glycine. Samples were then washed with PBS, resuspended in ChIP lysis buffer (0.5% SDS, 10 mM EDTA, 50 mM Tris-HCl at pH8), and sonicated (Bioruptor Plus, Diagenode) to release 100–1000 bp fragments. Samples were diluted 1:5 with ChIP dilution buffer (170 mM NaCl, 17 mM Tris-HCl at pH 8, 1.2 mM EDTA, 1.1% Triton X-100, 0.01% SDS). An antibody against NR1H3 (R&D Systems PP-PPZ0412-00, 4 µg per sample) or CEBPB (Santa Cruz Biotechnology sc-150X, 4 µg per sample) was conjugated to magnetic beads (Sera-Mag, Merck GE17152104010150) for 2 h at 4°C. Chromatin was immunoprecipitated with antibody-bead conjugates for 16 h at 4°C. Immunocomplexes were washed sequentially with the following buffers: low salt buffer (0.01% SDS, 1% Triton X-100, 2 mM EDTA, 20 mM Tris-HCl at pH 8, 150 mM NaCl), high salt buffer (0.01% SDS, 1% Triton X-100, 2 mM EDTA, 20 mM Tris-HCl at pH 8, 500 mM NaCl), LiCl buffer (0.25 M LiCl, 1% IGEPAL CA630, 1% deoxycholic acid, 1 mM EDTA, 10 mM Tris at pH 8.1), and twice with TE buffer (10 mM Tris-HCl, 1 mM EDTA at pH 8). Chromatin was eluted, de-cross-linked for 4 h at 65°C and deproteinized with Proteinase K (Hy Labs EPR9016) for 1 h at 50°C. DNA was subsequently isolated using a MinElute DNA purification kit (Qiagen 20-28006).

The sequences of primers used to validate NR1H3 ChIP efficiency and antibody specificity (Patel et al. 2017) are as follows:

Srebf1 LXRE—Fwd: CAGGCAACCATCCCCGAAA; Rev: ACAGAGC TTCCGGGATCAAAG.

Primary mouse hepatocytes

Primary hepatocytes were isolated from male, 8- to 10-week-old C57BL/6J mice. Isolation and plating of primary mouse hepatocytes were performed as detailed in our published protocol (Charni-Natan and Goldstein 2020). Three hours after plating, the media were changed to Williams' E media (Thermo Fisher Scientific 12551032). All treatments were performed 18 h after plating in Williams' E media. Treatments were added for 8 h (Glucagon 100 nM [Ray Biotech 228-10549-1], corticosterone 1 µM [Sigma-Aldrich 50-22-6], RU486 2 µM [Sigma-Aldrich M8046], GW3965 [1 µM, Cayman 10054], GSK2033 [10 µM, Sigma-Aldrich SML1617]) prior to RNA extraction.

For dominant-negative experiments, 3 h after plating primary mouse hepatocytes, adenoviruses containing a dominant negative peptide against CREB1 (Ahn et al. 1998; Korenfeld et al. 2021) or a control were added to the cultures (5×10^5 PFU/µL).

In shRNA adenovirus infection experiments, hepatocytes were infected with adenovirus (25,000 PFU/µL; shCEBPB Vector Biolabs shADV-255244) 3 h after plating.

For siRNA-mediated suppression of LXRs, 3 h after plating, primary mouse hepatocytes were transfected with pools of siRNA oligos targeting *Nr1h3* and *Nr1h2* (purchased from IDT) or with a negative control siRNA using Lipofectamine RNAiMAX (Thermo Fisher Scientific 13778075), according to the manufacturer's instructions. Following transfection, cells were treated as indicated and collected for RNA extraction 24 h after transfection.

The research has been approved by the Hebrew University of Jerusalem Institutional Animal Care and Use Committee with ethics approval numbers MD-22-17006 and MD-18-15596 (Jerusalem, Israel).

RNA-seq

Replicates were randomly selected from each experimental group and processed for RNA-seq. For quality control of RNA yield and library synthesis products, the RNA ScreenTape and D1000 ScreenTape kits (both from Agilent Technologies), Qubit RNA HS assay kit, and Qubit DNA HS assay kit (both from Invitrogen) were used. mRNA libraries were prepared from 1 µg RNA using the KAPA stranded mRNA-Seq kit, with mRNA capture beads (KAPA Biosystems KK8421). The multiplex sample pool (1.6 pM including PhiX 1%) was loaded on an Illumina sequencer.

ATAC-seq

Replicates were randomly selected from each experimental group and processed for ATAC-seq. ATAC-seq was performed as detailed in our freely accessible protocol (Korenfeld et al. 2023). Briefly, nuclei were isolated using a hypotonic buffer and Dounce homogenizer. Nuclei were tagmented using Tn5 transposase loaded with Illumina adapters. Tagmented DNA was PCR-amplified with sample-specific indices. The resulting library was size-selected to DNA fragments of 150–800 nt. The multiplex sample pool (1.6 pM including PhiX 1%) was loaded on an Illumina sequencer. Each sample was sequenced at a depth of at least 5×10^7 reads (paired-end).

Sequencing data analyses

FASTQ files were mapped to the GRCm38 (mm10) mouse genome assembly using Bowtie 2 (Langmead and Salzberg 2012) with default parameters. Tag directories were made using the

Downloaded from genome.cshlp.org on November 17, 2026 . Published by Cold Spring Harbor Laboratory Press

makeTagDirectory option in the HOMER suite (Heinz et al. 2010). For loci visualization, bedGraph files were generated for each biological replicate (using the makeUCSC file option in the HOMER suite). For normalization, the total number of reads in bedGraph files was set to 10^7. bedGraph files were then converted to TDF files by the Integrative Genomics Viewer (IGV) (Robinson et al. 2011). Then, selected gene loci were visualized using the IGV. The WT and DKO Refed raw data files originated from the same experiment previously published (Korenfeld et al. 2024). Of note, the Adlib-Fasted-Refed experiment described in Figure 1, including all nutritional states and genotypes, was performed together.

Differential gene expression

Differential gene expression was evaluated by DESeq2 (Love et al. 2014) via the HOMER suite under default parameters. Genes were determined as differentially expressed between two conditions if they passed these cutoffs: fold change ≥1.5, adjusted *P*-value ≤ 0.05.

Dimensionality reduction analysis

Principal component analysis (PCA) was performed in R using the "stats" package (prcomp function). The analyzed values are $\log_2(\text{RPKM}+1)$. Genes with RPKM < 0.5 were excluded.

Gene Ontology term enrichment analysis

Gene Ontology term enrichment analysis was performed by GeneAnalytics (Ben-Ari Fuchs et al. 2016).

ATAC-seq and ChIP-seq analyses

Peak-calling was performed by MACS2 (narrowPeak option) (Zhang et al. 2008). In ChIP-seq, the DKO sample was used as the control for MACS2. Differential enhancer accessibility was measured by DESeq2 (fold change ≥1.5, adj. *P* value ≤ 0.05). Genomic annotations were made by the HOMER suite (annotatePeaks option, parameter -annStats).

Motif enrichment analysis

Motif enrichment analysis was performed using the findMotifsGenome option in HOMER (parameter -size given). The motifs shown are the top 15 motifs with *P* value $\leq 1 \times 10^{-10}$ (option "known" in HOMER) In motif enrichment analyses of total ATAC accessible sites and of TF binding sites (NR1H3 and CEBPB), the background was automatically selected by HOMER to account for GC bias and other sequence biases. In LXR-regulated sites, the entire enhancer landscape (all ATAC accessible sites across all conditions) was used as the background to account for possible sequence bias. Using the entire enhancer landscape as the background ensures that prevalent motifs appearing across liver enhancers will not be falsely detected as specifically enriched in the examined subset of LXR-regulated enhancers.

Aggregate plots and box plots

Tag density of ATAC or ChIP signal was analyzed using the HOMER suite. In box plots, a tag count ±200 bp around the site center (averaged across all sites) was calculated using the HOMER suite: annotatePeaks, option -size 400 -noann. In all box plots, the 10–90 percentiles are plotted. In the H3K27 acetylation aggregate plot, the tag count (averaged across all sites) per site per base pair was calculated using the HOMER suite (annotatePeaks, option -size 8000 -hist 10). In both aggregate plot and box plots, the data are an average of all replicates.

Heatmaps

For each condition, tag directories from the three biological replicates were combined using the HOMER suite (makeTagDirectory). NR1H3 ChIP-seq tag density ±4 kb around the site center was calculated at all LXR-regulated sites across all nutritional states using HOMER (annotatePeaks option -size 8000 -hist 25 -ghist). The resulting matrices were visualized using Morpheus (https://software.broadinstitute.org/morpheus/) with a fixed color scale ranging from zero (white) to 1.2 (purple).

Motif distance

The distance between the center of the LXR motif and the center of the CEBP motif was measured in genomic regions in which both NR1H3 and CEBPB binding was detected in ChIP-seq across all nutritional states. The analysis includes only shared binding sites in which the consensus motifs of both TFs was found.

Data analyzed from the literature

The published transcriptome data sets that were obtained from the NCBI Gene Expression Omnibus (GEO; https://www.ncbi.nlm.nih.gov/geo/) and analyzed are as follows: GSE119713 (Kalvisa et al. 2018), GSE151546 (Kitamoto et al. 2021), GSE121096 (Ruppert et al. 2019), and GSE96559 (Régnier et al. 2018). NR3C1, CREB1, and H3K27 acetylation ChIP-seq data were retrieved from GSE72087 (Goldstein et al. 2017a). PPARA ChIP-seq data were retrieved from GSE118789 (Sommars et al. 2019). FOXO1 ChIP-seq data were retrieved from GSE119713 (Kalvisa et al. 2018).

Statistical analyses

Error bars represent the standard deviation of biological replicates. In pairwise comparisons, statistical significance was determined by a two-tailed, unpaired *t*-test. In comparisons of three or more groups, ordinary one-way or two-way ANOVA was performed, with post hoc analyses conducted using the Holm–Sidak test. In RNA-seq and ATAC-seq experiments, DESeq2 was used to determine statistical significance. (*) $P \leq 0.05$, (**) $P \leq 0.01$, (***) $P \leq 0.001$, (****) $P \leq 0.0001$, and (ns) $P > 0.05$.

Data access

All RNA-seq, ATAC-seq, and ChIP-seq data have been submitted to the NCBI Gene Expression Omnibus (GEO; https://www.ncbi.nlm.nih.gov/geo/) under accession number GSE305787.

Competing interest statement

The authors declare no competing interests.

Acknowledgments

This work was supported by the Canada-Israel Health Research Initiative, jointly funded by the Canadian Institutes of Health Research, the Israel Science Foundation, the International Development Research Centre, Canada, and the Azreili Foundation to I.G. (no. 1469/19, 3533/19) and C.L.C. (no. 109155-001) as well as the European Research Council to I.G. (ERC-StG no. 947907). We thank Dr. Abed Nasereddin and Dr. Idit Shiff from The Genomic Applications Lab, Hebrew University of Jerusalem, for their invaluable help, support, and expertise in high-throughput sequencing. We thank Michael Fadi Saikali (University of Toronto) for help in R analyses.

Downloaded from genome.cshlp.org on November 17, 2026 . Published by Cold Spring Harbor Laboratory Press

Author contributions: T.G. was involved in conceptualization, methodology, software, validation, formal analysis, writing, and investigation. M.C.R.F. was involved in investigation, methodology, validation, formal analysis, and visualization. H.S. was involved in investigation, methodology, validation, formal analysis, and visualization. N.K. was involved in investigation, methodology, validation, formal analysis, and visualization. C.S. was involved in investigation, methodology, validation, formal analysis, and visualization. S.A.S. was involved in investigation, methodology, validation, formal analysis, and visualization. D.G., T.R-F., M.A-B., and A.Y. were involved in investigation. M.C-N. was involved in methodology, software, validation, formal analysis, and investigation. M.B-S. was involved in project administration. C.L.C. was involved in conceptualization, methodology, formal analysis, investigation, resources, writing, visualization, supervision, project administration, and funding acquisition. I.G. was involved in conceptualization, methodology, software, validation, formal analysis, investigation, resources, writing, visualization, supervision, project administration, and funding acquisition.

References

Ahn S, Olive M, Aggarwal S, Krylov D, Ginty DD, Vinson C. 1998. A dominant-negative inhibitor of CREB reveals that it is a general mediator of stimulus-dependent transcription of c-*fos*. *Mol Cell Biol* **18:** 967–977. doi:10.1128/MCB.18.2.967

Anthonisen EH, Berven L, Holm S, Nygård M, Nebb HI, Grønning-Wang LM. 2010. Nuclear receptor liver X receptor is *O*-GlcNAc-modified in response to glucose. *J Biol Chem* **285:** 1607–1615. doi:10.1074/jbc.M109.082685

Barral A, Zaret KS. 2024. Pioneer factors: roles and their regulation in development. *Trends Genet* **40:** 134–148. doi:10.1016/j.tig.2023.10.007

Ben-Ari Fuchs S, Lieder I, Stelzer G, Mazor Y, Buzhor E, Kaplan S, Bogoch Y, Plaschkes I, Shitrit A, Rappaport N, et al. 2016. GeneAnalytics: an integrative gene set analysis tool for next generation sequencing, RNAseq and microarray data. *OMICS* **20:** 139–151. doi:10.1089/omi.2015.0168

Biddie SC, John S, Sabo PJ, Thurman RE, Johnson TA, Schiltz RL, Miranda TB, Sung MH, Trump S, Lightman SL, et al. 2011. Transcription factor AP1 potentiates chromatin accessibility and glucocorticoid receptor binding. *Mol Cell* **43:** 145–155. doi:10.1016/j.molcel.2011.06.016

Bideyan L, Nagari R, Tontonoz P. 2021. Hepatic transcriptional responses to fasting and feeding. *Genes Dev* **35:** 635–657. doi:10.1101/gad.348340.121

Bideyan L, Fan W, Kaczor-Urbanowicz KE, Priest C, Casero D, Tontonoz P. 2022. Integrative analysis reveals multiple modes of LXR transcriptional regulation in liver. *Proc Natl Acad Sci* **119:** e2122683119. doi:10.1073/pnas.2122683119

Boergesen M, Pedersen TA, Gross B, van Heeringen SJ, Hagenbeek D, Bindesbøll C, Caron S, Lalloyer F, Steffensen KR, Nebb HI, et al. 2012. Genome-wide profiling of liver X receptor, retinoid X receptor, and peroxisome proliferator-activated receptor α in mouse liver reveals extensive sharing of binding sites. *Mol Cell Biol* **32:** 852–867. doi:10.1128/MCB.06175-11

Calkin AC, Tontonoz P. 2012. Transcriptional integration of metabolism by the nuclear sterol-activated receptors LXR and FXR. *Nat Rev Mol Cell Biol* **13:** 213–224. doi:10.1038/nrm3312

Cariou B, van Harmelen K, Duran-Sandoval D, van Dijk T, Grefhorst A, Bouchaert E, Fruchart JC, Gonzalez FJ, Kuipers F, Staels B. 2005. Transient impairment of the adaptive response to fasting in FXR-deficient mice. *FEBS Lett* **579:** 4076–4080. doi:10.1016/j.febslet.2005.06.033

Carper D, Coué M, Laurens C, Langin D, Moro C. 2020. Reappraisal of the optimal fasting time for insulin tolerance tests in mice. *Mol Metab* **42:** 101058. doi:10.1016/j.molmet.2020.101058

Charni-Natan M, Goldstein I. 2020. Protocol for primary mouse hepatocyte isolation. *STAR Protoc* **1:** 100086. doi:10.1016/j.xpro.2020.100086

Defour M, Hooiveld G, van Weeghel M, Kersten S. 2020. Probing metabolic memory in the hepatic response to fasting. *Physiol Genomics* **52:** 602–617. doi:10.1152/physiolgenomics.00117.2020

Folch J, Lees M, Sloane Stanley GH. 1957. A simple method for the isolation and purification of total lipides from animal tissues. *J Biol Chem* **226:** 497–509. doi:10.1016/S0021-9258(18)64849-5

Fougerat A, Bruse J, Polizzi A, Montagner A, Guillou H, Wahli W. 2024. Lipid sensing by PPARα: role in controlling hepatocyte gene regulatory networks and the metabolic response to fasting. *Prog Lipid Res* **96:** 101303. doi:10.1016/j.plipres.2024.101303

Gasperini M, Tome JM, Shendure J. 2020. Towards a comprehensive catalogue of validated and target-linked human enhancers. *Nat Rev Genet* **21:** 292–310. doi:10.1038/s41576-019-0209-0

Glaría E, Martínez PR, Font-Díaz J, De la Rosa JV, Castrillo A, Crawshaw DJ, Vidal Taboada JM, Saura J, Matalonga J, Nunes Chini E, et al. 2025. Liver X receptors and inflammatory-induced C/EBPβ selectively cooperate to control CD38 transcription. *J Innate Immun* **17:** 56–77. doi:10.1159/000543274

Goldberg D, Goldstein I. 2026. Endocrine regulation of the hepatic fasting response: cues, cooperation and consequences. *Nat Rev Endocrinol* **22:** 302–316. doi:10.1038/s41574-025-01228-3

Goldberg D, Charni-Natan M, Buchshtab N, Bar-Shimon M, Goldstein I. 2022. Hormone-controlled cooperative binding of transcription factors drives synergistic induction of fasting-regulated genes. *Nucleic Acids Res* **50:** 5528–5544. doi:10.1093/nar/gkac358

Goldberg D, Buchshtab N, Charni-Natan M, Goldstein I. 2024. Transcriptional cascades during fasting amplify gluconeogenesis and instigate a secondary wave of ketogenic gene transcription. *Liver Int* **44:** 2964–2982. doi:10.1111/liv.16077

Goldstein I. 2020. Chromatin regulation and transcription factor cooperation in liver cells. In *The liver* (ed. Arias HJA, et al.), pp. 1043–1049. Wiley, Hoboken, NJ.

Goldstein I, Hager GL. 2015. Transcriptional and chromatin regulation during fasting - the genomic era. *Trends Endocrinol Metab* **26:** 699–710. doi:10.1016/j.tem.2015.09.005

Goldstein I, Hager GL. 2018. The three Ds of transcription activation by glucagon: direct, delayed, and dynamic. *Endocrinology* **159:** 206–216. doi:10.1210/en.2017-00521

Goldstein I, Baek S, Presman DM, Paakinaho V, Swinstead EE, Hager GL. 2017a. Transcription factor assisted loading and enhancer dynamics dictate the hepatic fasting response. *Genome Res* **27:** 427–439. doi:10.1101/gr.212175.116

Goldstein I, Paakinaho V, Baek S, Sung MH, Hager GL. 2017b. Synergistic gene expression during the acute phase response is characterized by transcription factor assisted loading. *Nat Commun* **8:** 1849. doi:10.1038/s41467-017-02055-5

Grøntved L, John S, Baek S, Liu Y, Buckley JR, Vinson C, Aguilera G, Hager GL. 2013. C/EBP maintains chromatin accessibility in liver and facilitates glucocorticoid receptor recruitment to steroid response elements. *EMBO J* **32:** 1568–1583. doi:10.1038/emboj.2013.106

Heckmann BL, Zhang X, Saarinen AM, Schoiswohl G, Kershaw EE, Zechner R, Liu J. 2017. Liver X receptor α mediates hepatic triglyceride accumulation through upregulation of G0/G1 switch gene 2 expression. *JCI Insight* **2:** e88735. doi:10.1172/jci.insight.88735

Heinz S, Benner C, Spann N, Bertolino E, Lin YC, Laslo P, Cheng JX, Murre C, Singh H, Glass CK. 2010. Simple combinations of lineage-determining transcription factors prime *cis*-regulatory elements required for macrophage and B cell identities. *Mol Cell* **38:** 576–589. doi:10.1016/j.molcel.2010.05.004

Heinz S, Romanoski CE, Benner C, Glass CK. 2015. The selection and function of cell type-specific enhancers. *Nat Rev Molecular Cell Biolo* **16:** 144–154. doi:10.1038/nrm3949

Hiltunen J, Helminen L, Aaltonen N, Launonen KM, Laakso H, Malinen M, Niskanen EA, Palvimo JJ, Paakinaho V. 2025. Androgen receptor-mediated assisted loading of the glucocorticoid receptor modulates transcriptional responses in prostate cancer cells. *Genome Res* **35:** 1717–1732. doi:10.1101/gr.280224.124

Hunter AL, Poolman TM, Kim D, Gonzalez FJ, Bechtold DA, Loudon ASI, Iqbal M, Ray DW. 2022. HNF4A modulates glucocorticoid action in the liver. *Cell Rep* **39:** 110697. doi:10.1016/j.celrep.2022.110697

Janowski BA, Willy PJ, Devi TR, Falck JR, Mangelsdorf DJ. 1996. An oxysterol signalling pathway mediated by the nuclear receptor LXRα. *Nature* **383:** 728–731. doi:10.1038/383728a0

Kalvisa A, Siersbaek MS, Praestholm SM, Christensen LJL, Nielsen R, Stohr O, Vettorazzi S, Tuckermann J, White M, Mandrup S, et al. 2018. Insulin signaling and reduced glucocorticoid receptor activity attenuate postprandial gene expression in liver. *PLoS Biol* **16:** e2006249. doi:10.1371/journal.pbio.2006249

Kersten S. 2014. Integrated physiology and systems biology of PPARα. *Mol Metab* **3:** 354–371. doi:10.1016/j.molmet.2014.02.002

Kitamoto T, Kuo T, Okabe A, Kaneda A, Accili D. 2021. An integrative transcriptional logic model of hepatic insulin resistance. *Proc Natl Acad Sci* **118:** e2102222118. doi:10.1073/pnas.2102222118

Korach-André M, Parini P, Larsson L, Arner A, Steffensen KR, Gustafsson JA. 2010. Separate and overlapping metabolic functions of LXRα and LXRβ in C57Bl/6 female mice. *Am J Physiol Endocrinol Metab* **298:** E167–E178. doi:10.1152/ajpendo.00184.2009

Korenfeld N, Finkel M, Buchshtab N, Bar-Shimon M, Charni-Natan M, Goldstein I. 2021. Fasting hormones synergistically induce amino acid

Downloaded from genome.cshlp.org on November 17, 2026 . Published by Cold Spring Harbor Laboratory Press

catabolism genes to promote gluconeogenesis. *Cell Mol Gastroenterol Hepatol* **12:** 1021–1036. doi:10.1016/j.jcmgh.2021.04.017
Korenfeld N, Toft NI, Dam TV, Charni-Natan M, Grøntved L, Goldstein I. 2023. Protocol for bulk and single-nuclei chromatin accessibility quantification in mouse liver tissue. *STAR Protoc* **4:** 102462. doi:10.1016/j.xpro.2023.102462
Korenfeld N, Gorbonos T, Romero Florian MC, Rotaro D, Goldberg D, Radushkevitz-Frishman T, Charni-Natan M, Bar-Shimon M, Cummins CL, Goldstein I. 2024. LXR-dependent enhancer activation regulates the temporal organization of the liver's response to refeeding leading to lipogenic gene overshoot. *PLoS Biol* **22:** e3002735. doi:10.1371/journal.pbio.3002735
Langmead B, Salzberg SL. 2012. Fast gapped-read alignment with Bowtie 2. *Nat Methods* **9:** 357–359. doi:10.1038/nmeth.1923
Lee JH, Sánchez-Rivera FJ, He L, Basnet H, Chen FX, Spina E, Li L, Torner C, Chan JE, Yarlagadda DVK, et al. 2024. TGF-β and RAS jointly unmask primed enhancers to drive metastasis. *Cell* **187:** 6182–6199.e29. doi:10.1016/j.cell.2024.08.014
Liang G, Yang J, Horton JD, Hammer RE, Goldstein JL, Brown MS. 2002. Diminished hepatic response to fasting/refeeding and liver X receptor agonists in mice with selective deficiency of sterol regulatory element-binding protein-1c. *J Biol Chem* **277:** 9520–9528. doi:10.1074/jbc.M111421200
Liu S, Croniger C, Arizmendi C, Harada-Shiba M, Ren J, Poli V, Hanson RW, Friedman JE. 1999. Hypoglycemia and impaired hepatic glucose production in mice with a deletion of the C/EBPβ gene. *J Clin Invest* **103:** 207–213. doi:10.1172/JCI4243
Love MI, Huber W, Anders S. 2014. Moderated estimation of fold change and dispersion for RNA-seq data with DESeq2. *Genome Biol* **15:** 550. doi:10.1186/s13059-014-0550-8
Madsen MS, Siersbæk R, Boergesen M, Nielsen R, Mandrup S. 2014. Peroxisome proliferator-activated receptor γ and C/EBPα synergistically activate key metabolic adipocyte genes by assisted loading. *Mol Cell Biol* **34:** 939–954. doi:10.1128/MCB.01344-13
Nason SR, Kim T, Antipenko JP, Finan B, DiMarchi R, Hunter CS, Habegger KM. 2020. Glucagon-receptor signaling reverses hepatic steatosis independent of leptin receptor expression. *Endocrinology* **161:** bqz013. doi:10.1210/endocr/bqz013
Oosterveer MH, van Dijk TH, Grefhorst A, Bloks VW, Havinga R, Kuipers F, Reijngoud DJ. 2008. *Lxr*α deficiency hampers the hepatic adaptive response to fasting in mice. *J Biol Chem* **283:** 25437–25445. doi:10.1074/jbc.M801922200
Patel R, Patel M, Tsai R, Lin V, Bookout AL, Zhang Y, Magomedova L, Li T, Chan JF, Budd C, et al. 2011. LXRβ is required for glucocorticoid-induced hyperglycemia and hepatosteatosis in mice. *J Clin Invest* **121:** 431–441. doi:10.1172/JCI41681
Patel R, Magomedova L, Tsai R, Angers S, Orellana A, Cummins CL. 2017. Separating the anti-inflammatory and diabetogenic effects of glucocorticoids through LXRβ antagonism. *Endocrinology* **158:** 1034–1047. doi:10.1210/en.2017-00094
Peet DJ, Turley SD, Ma W, Janowski BA, Lobaccaro JM, Hammer RE, Mangelsdorf DJ. 1998. Cholesterol and bile acid metabolism are impaired in mice lacking the nuclear oxysterol receptor LXRalpha. *Cell* **93:** 693–704. doi:10.1016/S0092-8674(00)81432-4
Præstholm SM, Correia CM, Grøntved L. 2020a. Multifaceted control of GR signaling and its impact on hepatic transcriptional networks and metabolism. *Front Endocrinol (Lausanne)* **11:** 572981. doi:10.3389/fendo.2020.572981
Præstholm SM, Siersbæk MS, Nielsen R, Zhu X, Hollenberg AN, Cheng SY, Grøntved L. 2020b. Multiple mechanisms regulate H3 acetylation of enhancers in response to thyroid hormone. *PLoS Genet* **16:** e1008770. doi:10.1371/journal.pgen.1008770
Quagliarini F, Mir AA, Balazs K, Wierer M, Dyar KA, Jouffe C, Makris K, Hawe J, Heinig M, Filipp FV, et al. 2019. Cistromic reprogramming of the diurnal glucocorticoid hormone response by high-fat diet. *Mol Cell* **76:** 531–545.e5. doi:10.1016/j.molcel.2019.10.007
Quinet EM, Savio DA, Halpern AR, Chen L, Schuster GU, Gustafsson JA, Basso MD, Nambi P. 2006. Liver X receptor (LXR)-β regulation in LXRα-deficient mice: implications for therapeutic targeting. *Mol Pharmacol* **70:** 1340–1349. doi:10.1124/mol.106.022608
Rahman SM, Choudhury M, Janssen RC, Baquero KC, Miyazaki M, Friedman JE. 2013. CCAAT/enhancer binding protein β deletion increases mitochondrial function and protects mice from LXR-induced hepatic steatosis. *Biochem Biophys Res Commun* **430:** 336–339. doi:10.1016/j.bbrc.2012.11.027
Ramón-Vázquez A, de la Rosa JV, Tabraue C, Lopez F, Díaz-Chico BN, Bosca L, Tontonoz P, Alemany S, Castrillo A. 2019. Common and differential transcriptional actions of nuclear receptors liver X receptors α and β in macrophages. *Mol Cell Biol* **39:** e00376-18. doi:10.1128/MCB.00376-18
Régnier M, Polizzi A, Lippi Y, Fouché E, Michel G, Lukowicz C, Smati S, Marrot A, Lasserre F, Naylies C, et al. 2018. Insights into the role of hepatocyte PPARα activity in response to fasting. *Mol Cell Endocrinol* **471:** 75–88. doi:10.1016/j.mce.2017.07.035
Repa JJ, Liang G, Ou J, Bashmakov Y, Lobaccaro JM, Shimomura I, Shan B, Brown MS, Goldstein JL, Mangelsdorf DJ. 2000. Regulation of mouse sterol regulatory element-binding protein-1c gene (SREBP-1c) by oxysterol receptors, LXRα and LXRβ. *Genes Dev* **14:** 2819–2830. doi:10.1101/gad.844900
Robinson JT, Thorvaldsdóttir H, Winckler W, Guttman M, Lander ES, Getz G, Mesirov JP. 2011. Integrative genomics viewer. *Nat Biotechnol* **29:** 24–26. doi:10.1038/nbt.1754
Roesler WJ. 2001. The role of C/EBP in nutrient and hormonal regulation of gene expression. *Annu Rev Nutr* **21:** 141–165. doi:10.1146/annurev.nutr.21.1.141
Rong S, Cortés VA, Rashid S, Anderson NN, McDonald JG, Liang G, Moon YA, Hammer RE, Horton JD. 2017. Expression of SREBP-1c requires SREBP-2-mediated generation of a sterol ligand for LXR in livers of mice. *eLife* **6:** e25015. doi:10.7554/eLife.25015
Ruppert PMM, Park JG, Xu X, Hur KY, Lee AH, Kersten S. 2019. Transcriptional profiling of PPARα$^{-/-}$ and CREB3L3$^{-/-}$ livers reveals disparate regulation of hepatoproliferative and metabolic functions of PPARα. *BMC Genomics* **20:** 199. doi:10.1186/s12864-019-5563-y
Secor SM, Carey HV. 2016. Integrative physiology of fasting. *Compr Physiol* **6:** 773–825. doi:10.1002/j.2040-4603.2016.tb00693.x
Seuter S, Neme A, Carlberg C. 2017. Epigenomic PU.1-VDR crosstalk modulates vitamin D signaling. *Biochim Biophys Acta Gene Regul Mech* **1860:** 405–415. doi:10.1016/j.bbagrm.2017.02.005
Smati S, Polizzi A, Fougerat A, Ellero-Simatos S, Blum Y, Lippi Y, Régnier M, Laroyenne A, Huillet M, Arif M, et al. 2022. Integrative study of diet-induced mouse models of NAFLD identifies PPARα as a sexually dimorphic drug target. *Gut* **71:** 807–821. doi:10.1136/gutjnl-2020-323323
Sommars MA, Ramachandran K, Senagolage MD, Futtner CR, Germain DM, Allred AL, Omura Y, Bederman IR, Barish GD. 2019. Dynamic repression by BCL6 controls the genome-wide liver response to fasting and steatosis. *eLife* **8:** e43922. doi:10.7554/eLife.43922
Swinstead EE, Miranda TB, Paakinaho V, Baek S, Goldstein I, Hawkins M, Karpova TS, Ball D, Mazza D, Lavis LD, et al. 2016a. Steroid receptors reprogram FoxA1 occupancy through dynamic chromatin transitions. *Cell* **165:** 593–605. doi:10.1016/j.cell.2016.02.067
Swinstead EE, Paakinaho V, Presman DM, Hager GL. 2016b. Pioneer factors and ATP-dependent chromatin remodeling factors interact dynamically: a new perspective: multiple transcription factors can effect chromatin pioneer functions through dynamic interactions with ATP-dependent chromatin remodeling factors. *Bioessays* **38:** 1150–1157. doi:10.1002/bies.201600137
Tian J, Goldstein JL, Brown MS. 2016. Insulin induction of SREBP-1c in rodent liver requires LXRα-C/EBPβ complex. *Proc Natl Acad Sci* **113:** 8182–8187. doi:10.1073/pnas.1608987113
Torra IP, Ismaili N, Feig JE, Xu CF, Cavasotto C, Pancratov R, Rogatsky I, Neubert TA, Fisher EA, Garabedian MJ. 2008. Phosphorylation of liver X receptor α selectively regulates target gene expression in macrophages. *Mol Cell Biol* **28:** 2626–2636. doi:10.1128/MCB.01575-07
Voisin M, Gage MC, Becares N, Shrestha E, Fisher EA, Pineda-Torra I, Garabedian MJ. 2020. LXRα phosphorylation in cardiometabolic disease: insight from mouse models. *Endocrinology* **161:** bqaa089. doi:10.1210/endocr/bqaa089
Wang B, Tontonoz P. 2018. Liver X receptors in lipid signalling and membrane homeostasis. *Nat Rev Endocrinol* **14:** 452–463. doi:10.1038/s41574-018-0037-x
Wong S, Tan K, Carey KT, Fukushima A, Tiganis T, Cole TJ. 2010. Glucocorticoids stimulate hepatic and renal catecholamine inactivation by direct rapid induction of the dopamine sulfotransferase Sult1d1. *Endocrinology* **151:** 185–194. doi:10.1210/en.2009-0590
Xu C, Kleinschmidt H, Yang J, Leith EM, Johnson J, Tan S, Mahony S, Bai L. 2024. Systematic dissection of sequence features affecting binding specificity of a pioneer factor reveals binding synergy between FOXA1 and AP-1. *Mol Cell* **84:** 2838–2855.e10. doi:10.1016/j.molcel.2024.06.022
Zhang Y, Liu T, Meyer CA, Eeckhoute J, Johnson DS, Bernstein BE, Nusbaum C, Myers RM, Brown M, Li W, et al. 2008. Model-based Analysis of ChIP-Seq (MACS). *Genome Biol* **9:** R137. doi:10.1186/gb-2008-9-9-r137
Zhang Y, Breevoort SR, Angdisen J, Fu M, Schmidt DR, Holmstrom SR, Kliewer SA, Mangelsdorf DJ, Schulman IG. 2012. Liver LXRα expression is crucial for whole body cholesterol homeostasis and reverse cholesterol transport in mice. *J Clin Invest* **122:** 1688–1699. doi:10.1172/JCI59817

Received March 16, 2026; accepted in revised form October 6, 2026.